Cancer Biol Med 2026. doi: 10.20892/j.issn.2095-3941.2026.0168

ORIGINAL ARTICLE

OPEN ACCESS

Myeloid cell reprogramming combined with zoledronic acid effectively suppresses bone metastasis

Yuting Luo, Yiran Cai, Zizheng Jiang, Ke Zheng, Shiji Ren, Lixia Yu, Baorui Liu, Tao Shi, Jia Wei

Department of Oncology, Nanjing Drum Tower Hospital, Affiliated Hospital of Medical School, Nanjing University, Nanjing 210008, China

ABSTRACT

Objective: Bone metastases are refractory to current therapies, primarily owing to the immunosuppressive metastasis tumor microenvironment (TME), which is dominated by myeloid cells. However, the function and regulatory mechanisms of myeloid compartments within the bone TME are incompletely understood. Herein we sought to delineate the role of the DKK1-CKAP4 axis in shaping myeloid cell-mediated immunosuppression in bone metastases and to identify potential therapeutic strategies targeting this pathway.

Methods: The composition and phenotypic characteristics of myeloid cells in the bone TME were analyzed. Mechanistic studies were conducted using *ex vivo* co-culture systems and an *in vivo* *Ckap4*$^{fl/fl}$*S100a8*^{Cre} (neutrophil-specific *Ckap4* knockout) mouse model to delineate the role of the DKK1-CKAP4 axis in regulating neutrophil maturation, osteoclast-like cell differentiation, and macrophage polarization. The therapeutic efficacy of DKK1 blockade in combination with zoledronic acid, as well as the impact on remodeling the TME, was further validated in bone metastasis mouse models.

Results: Significant expansion and predominance of myeloid cells within the bone TME was noted. Mechanistically, the DKK1-CKAP4 axis regulated the development and function of multiple myeloid populations. The DKK1-CKAP4 axis drove neutrophils toward an immature-like, immunosuppressive phenotype, promoted osteoclast-like cell differentiation, and induced macrophage polarization into an M2-like phenotype. Importantly, combined therapy with DKK1 blockade and zoledronic acid reprogrammed immunosuppressive myeloid cells, restored antitumor immunity, and significantly reduced tumor burden in bone metastasis models.

Conclusions: The findings herein showed the DKK1-CKAP4 axis to be a key regulator of myeloid-driven immunosuppression in the bone TME. The combination of DKK1 blockade with zoledronic acid represents a potential therapeutic strategy for bone metastases.

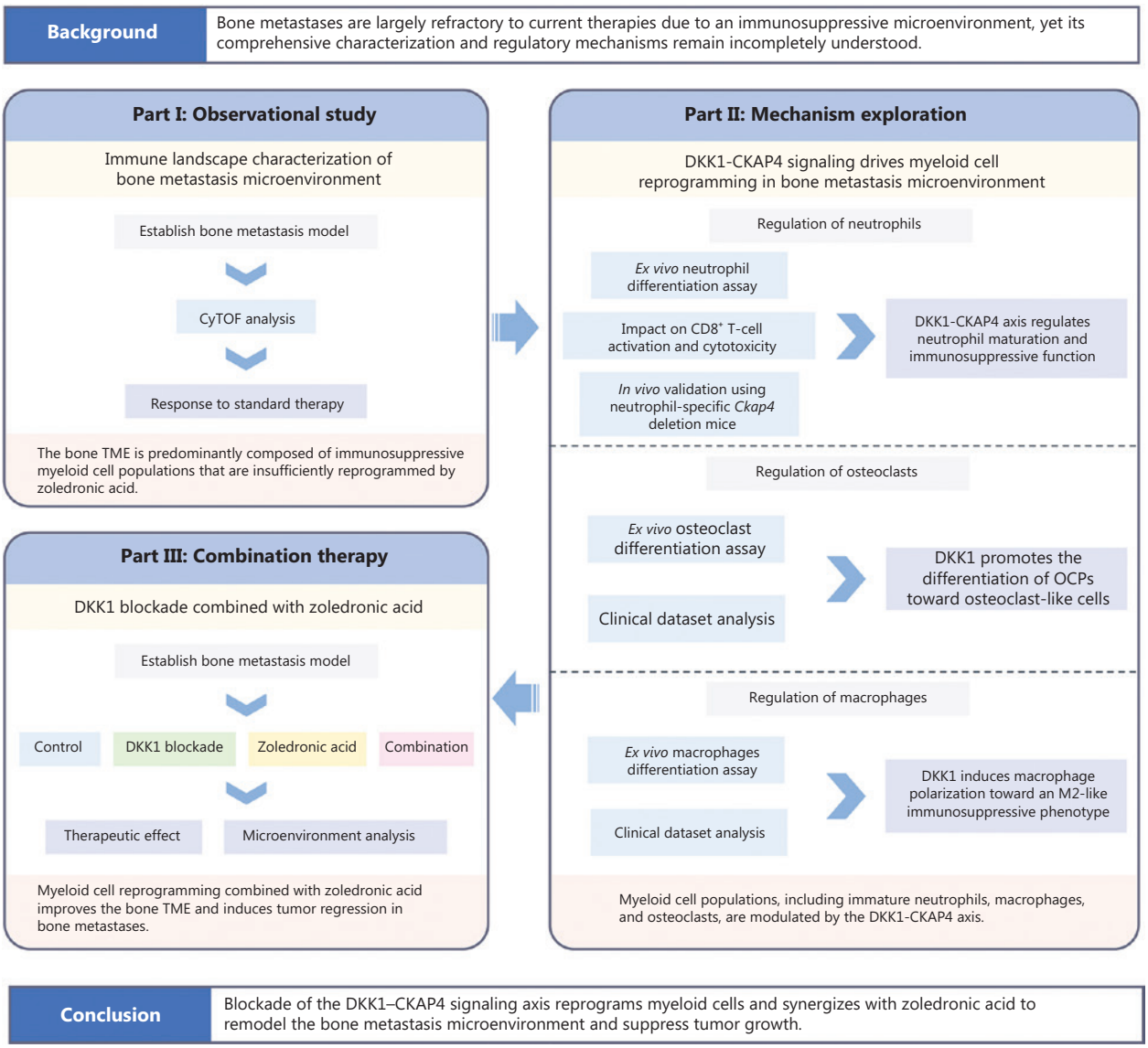
KEYWORDS Bone metastasis; myeloid cell reprogramming; DKK1-CKAP4 axis; zoledronic acid; combination cancer therapy

Introduction

Bone is a common site of metastasis for various solid tumors, including breast, prostate, and lung cancers[1,2]. Bone metastases are frequently accompanied by severe skeletal-related events (SREs), such as pathologic fractures, intractable bone pain, and hypercalcemia, which threaten the quality of life and survival of bone-metastatic cancer patients[3,4]. Despite the significant morbidity and mortality associated with bone metastases, traditional therapies, including chemotherapy and radiotherapy, provide limited clinical benefit when compared to the efficacy against primary tumors[5]. In current clinical practice, bone-targeted agents (BTAs), including bisphosphonates (e.g., zoledronic acid), are routinely used as standard therapy for patients with bone metastases[6]. These agents exert effects predominantly through suppression of osteoclast-dependent bone degradation, thereby preserving bone integrity and preventing SREs[7-12]. Immunotherapies, such as immune checkpoint blockade (ICB), have shown promising efficacy in various solid tumors. However, the therapeutic responses in bone metastases are unsatisfactory, owing to the unique bone metastases microenvironment[13-17].

Myeloid cells are the predominant population in the bone metastatic niche, shaping a profoundly immunosuppressive microenvironment[18]. Among the myeloid cells, neutrophils constitute the largest myeloid subset within the bone marrow microenvironment. Tumor-associated neutrophils (TANs) have gained considerable attention for their dual roles in the tumor microenvironment (TME), where they mediate crosstalk between tumor cells and other immune components, such as T cells, macrophages, and dendritic cells (DCs), thereby significantly influencing the response to immunotherapy[19,20].

Correspondence to: Tao Shi and Jia Wei
E-mail: taoshi@smail.nju.edu.cn and jiawei99@nju.edu.cn
ORCID ID: https://orcid.org/0000-0002-9825-3983 and https://orcid.org/0000-0003-3024-8878
Received February 25, 2026; accepted June 3, 2026;
published online July 27, 2026.
Available at www.cancerbiomed.org
©2026 The Authors. Creative Commons Attribution-NonCommercial 4.0 International License (CC BY-NC 4.0)



Study Flowchart In Part I the immune landscape of bone metastasis was characterized by CyTOF analysis of bone marrow CD45$^+$ immune cells from tumor-bearing and healthy mice. The therapeutic efficacy of zoledronic acid was evaluated by measuring tumor burden and immune changes in the bone microenvironment. The bone TME was dominated by expanded immunosuppressive myeloid populations and zoledronic acid alone failed to effectively reprogram the myeloid compartment or suppress tumor progression. In Part II mechanisms underlying myeloid reprogramming was investigated using *ex vivo* co-culture assays, neutrophil-specific *Ckap4* deletion mouse models, and integrative clinical database analyses, which showed that the DKK1-CKAP4 signaling axis impairs neutrophil maturation, promotes the differentiation of OCPs toward osteoclast-like cells, and drives macrophage polarization in the bone TME. In Part III the combination of DKK1 blockade and zoledronic acid was shown to remodel the bone metastatic immune microenvironment, inhibits tumor progression, and enhance antitumor immunity. CyTOF, mass cytometry; DKK1, Dickkopf-related protein 1; CKAP4, cytoskeleton-associated protein 4; OCP, osteoclast precursor cell. Figure created with Microsoft PowerPoint.

Our recent work has shown that immature TANs have a critical impact on bone metastasis progression by fostering an immunosuppressive microenvironment[21]. In addition, emerging evidence highlights the multiple pro-tumor functions of osteoclasts in bone metastases. Beyond the classical function in bone resorption and facilitating tumor colonization, osteoclasts can reshape both local and distant microenvironments to promote metastatic progression[22-24]. Moreover, macrophages are highly enriched in the bone TME, where macrophages exert immunosuppressive effects and drive therapeutic resistance through

both microenvironmental regulation and direct interactions with tumor cells[25,26]. Despite these findings, the mechanisms underlying immune resistance in the bone TME are poorly understood. Therefore, it is imperative to further elucidate the function of myeloid cells in the bone metastasis microenvironment and to identify potential therapeutic targets.

Dickkopf-1 (DKK1), a secreted glycoprotein that antagonizes Wnt/β-catenin signaling, exerts tumor-promoting and immunomodulatory functions by engaging its receptor cytoskeleton-associated protein 4 (CKAP4)[27-29]. CKAP4 is widely expressed on various tumor cells and is also prominently present on myeloid cells within the TME[28,29]. In multiple tumor contexts, elevated DKK1 binds to CKAP4 on tumor cells and promotes tumor cell migration and proliferation[27,30-32]. In addition to these tumor-intrinsic functions, CKAP4 expression on myeloid immune cells enables the DKK1-CKAP4 axis to modulate the TME by promoting the recruitment and polarization of immunosuppressive myeloid populations[33-35]. DKK1 is predominantly secreted by osteoblasts and osteocytes, resulting in high concentrations in the bone marrow niche[21]. Clinically, elevated DKK1 levels in tumors and serum are associated with bone metastases in breast, lung, and prostate cancers[36-38]. These studies suggested that DKK1-CKAP4 signaling may have a profound impact on the immune landscape during bone metastases. However, the specific role of the DKK1-CKAP4 axis in the bone metastasis microenvironment and its potential as a therapeutic target are unclear.

In this study the profound impact of myeloid populations in the bone TME was identified, including immature neutrophils, activated osteoclasts, and immunosuppressive macrophages. These myeloid populations are reprogrammed by the DKK1-CKAP4 axis toward a more immunosuppressive phenotype. Moreover, combining myeloid cell reprogramming with zoledronic acid exerts potent antitumor effects and reshapes the bone metastasis microenvironment (see **Study Flowchart**).

Materials and methods

Cell line

The 4T1 cell line, a triple-negative mammary carcinoma originating from Balb/c mice, and the Lewis lung carcinoma (LLC) cell line, a Lewis lung carcinoma originating from C57BL/6 mice, were acquired from the National Collection of Authenticated Cell Cultures (Shanghai, China). Both cell lines were cultured in RPMI-1640 complete medium (Gibco, Grand Island, NY, USA), as previously described[21].

Mice

BALB/c and C57BL/6 mice were used in this study. These animals were acquired from the Institute of Hematology, Chinese Academy of Medical Sciences (Tianjin, China). C57BL/6JGpt-*Ckap4*^{em1Cflox}/Gpt (*Ckap4*$^{fl/fl}$) and *Ckap4*$^{fl/fl}$*S100a8*^{cre} mice were provided by GemPharmatech Co., Ltd (Nanjing, China). Six- to eight-week-old female mice were randomly divided into experimental groups for *in vivo* experiments. The Institutional Animal Care and Use Committee of Drum Tower Hospital approved all animal procedures (approval No. 2020AE01064).

Human data analysis

Transcriptomic data of metastatic samples from breast cancer patients were obtained from the Gene Expression Omnibus (GEO) database [GSE14018 (n = 58), GSE14020 (n = 65), and GSE54323 (n = 18)]. DKK1 mRNA expression in bone metastases was compared to metastases at other sites. It should be noted that GSE14020 integrates samples originally derived from GSE14018 and GSE14017. Owing to the batch effect adjustment and normalization performed during data merging, DKK1 expression in GSE14020 may exhibit minor discrepancies compared to the original GSE14018 series. Gene set enrichment analysis (GSEA) was performed to explore the relationship between DKK1 expression and bone-related biological pathways. Spearman's rank correlation was used to examine the associations between DKK1 and several immune- or myeloid-related markers (CCL20, CCL7, CXCL5, S100A8, S100A9, and TNFRSF14).

Single-cell RNA sequencing (scRNA-seq) data (GSE143791) were used. This dataset was comprised of the following bone marrow samples: bone metastatic prostate tumors (tumor site); uninvolved bone marrow (distal); and bone marrow from cancer-free orthopedic patients (benign). Quality control, normalization, and batch effect correction were performed following standard pipelines. Dimensionality reduction and cell clustering were performed using t-distributed stochastic neighbor embedding (t-SNE) to visualize the major immune cell subsets (B cell, myeloid cell, NK cell, plasma cell, and T cell) with the myeloid cell compartment, including monocytes, macrophages, neutrophils, osteoclasts, and DCs. *CKAP4* expression was examined across all cells as well as within the myeloid cell subset and a feature plot was generated to illustrate the distribution of *CKAP4* expression. Myeloid cells in the tumor site group were divided into *CKAP4*-high and -low subgroups based on *CKAP4* expression. Signature scores were calculated for each subgroup and compared to the following gene sets: immunosuppression-related genes (*LGALS9*, *LILRB3*, *LILRB2*, *HIF1A*, *CD44*, *CD47*, *PTPN2*, *TGIF1*, and *S100A8*) and antigen presentation-related genes (*HLA-DRA*, *HLA-DPB1*, *HLA-B*, *HLA-A*, *PSMB9*, *PSMB8*, *CTSS*, *CTSB*, and *CLEC7A*).

In vivo experiments

Construction and treatment of bone metastases models

4T1 cells were resuspended in phosphate-buffered saline (PBS) (2×10^6 cells/mL) to establish the 4T1 bone metastasis model

and 100 μL of the cell suspension was administered into the caudal artery (CA) of BALB/c mice. LLC cells were prepared in PBS (5×10^6 cells/mL) for the LLC bone metastases model and 100 μL of the suspension was administered into the CA of C57BL/6 mice.

After tumor inoculation, mice were randomly divided to receive intraperitoneal (i.p.) treatment with one of the following regimens: mouse monoclonal DKK1 antibody [αDKK1] (10 mg/kg once every 3 d; Leap Therapeutics, Cambridge, MA, USA); IgG2a isotype control [C1.18.4 (10 mg/kg once every 3 d); BioXCell, Lebanon, NH, USA]; zoledronic acid (100 μg/kg once weekly; Sigma, St. Louis, MO, USA); or a combination of αDKK1 and zoledronic acid. The body weights of mice from different groups were recorded during the treatment schedule.

Generation of Ckap4$^{fl/fl}$S100a8^{cre} mice

The *Ckap4*$^{fl/fl}$ mouse line (C57BL/6JGpt-*Ckap4*^{em1Cflox}/Gpt) was generated by (GemPharmatech, Nanjing, China). *Ckap4*$^{flox/flox}$ mice were crossed with a transgenic line expressing Cre recombinase under the control of the *S100a8* promoter [C57BL/6JGpt-H11$^{em1Cin(hS100a8\text{-}iCre)}$/Gpt; *S100a8*^{cre}] to generate mice with neutrophil-specific deletion of *Ckap4*. Genotyping results confirming the expected recombination are presented in **Figure S1**.

Magnetic resonance imaging (MRI) analysis

Tumor burden was assessed by MRI on day 21 using a BioSpec 7T system (Bruker BioSpin, Billerica, MA, USA). Bone metastases in the hind limbs of mice treated with IgG2a, zoledronic acid, αDKK1, or the combination of αDKK1 and zoledronic acid were visualized and images were evaluated with RadiAnt DICOM Viewer (2020.1).

Histologic analysis

Mice were sacrificed at the experimental endpoint and the femurs were harvested. The bone samples were fixed, decalcified, dehydrated, embedded, and sectioned (5 μm), as previously described[21]. Bone lesions were then stained with hematoxylin and eosin (H&E) or tartrate-resistant acid phosphatase (TRAP). The number of TRAP-positive cells per millimeter of bone interphase was quantified using Image-Pro Plus 6.0 (Media Cybernetics, Rockville, MD, USA).

Flow cytometry analysis

Bone marrow from mice in each group was immediately collected at the experimental endpoint. Cells were harvested from the tibias and femurs by centrifugation, then passed through 40-μm nylon strainers (Biosharp, Hefei, China). Erythrocytes were depleted using red blood cell lysis buffer (Biosharp), followed by two additional PBS washes. Prior to surface marker staining, cells were subjected to viability dye staining (BioLegend, San Diego, CA, USA) and Fc receptor blocking (BioLegend) following recently published protocols[39]. Single-cell suspensions were stained with the corresponding mouse antibodies for 30 min at 4°C, then washed twice with PBS for detection of cell surface markers [CD3, CD8, CD11b, CD11c, F4/80, CD80, CD86, CD163, Gr-1, MHC-II, NKp46, CD25, CD69, CD107a, Ly6G, CD101, and CKAP4] (BioLegend). Intracellular staining for CD206, Arg1, and iNOS was performed using anti-mouse antibody in combination with the Fixation/Permeabilization Solution Kit (BD Biosciences, San Jose, CA, USA). Stained cells were analyzed on a BD Accuri C6 PLUS flow cytometer (BD Biosciences) and all raw data were analyzed with FlowJo software (version 10.4; Tree Star, Ashland, OR, USA).

Ex vivo experiments

Mass cytometry (CyTOF) analysis

Bone marrow samples were collected from 3 healthy BALB/c mice (6–8 weeks old) and 3 BALB/c mice bearing 4T1 bone metastases. Single-cell suspensions were prepared, followed by red blood cell lysis. CD45$^+$ immune cells were subsequently isolated through fluorescence-activated cell sorting (FACS) and pooled into one sample per group. For each sample, approximately 3.5×10^5 CD45$^+$ cells were sorted and submitted for CyTOF analysis (PLT TECH, Hangzhou, China). After data acquisition, a total of 232,232 CD45$^+$ cells from healthy mice and 287,458 CD45$^+$ cells from bone metastasis-bearing mice were retained for downstream analysis. Cells were stained using a panel of metal-conjugated antibodies targeting surface and intracellular markers, including CD45, CD3e, Ki67, CD117, MHC-II, Granzyme B, CX3CR1, CD163, CD38, Ly6G, Ly6C, CD19, CD127, CD62L, CD11c, CD44, CD24, CD103, Gr-1, FcεRIα, TCRγδ, F4/80, TCRβ, CD64, CD69, CD25, CD86, NK1.1, CD27, CD206, FOXP3, CD137, T-bet, and CD80. Following staining, cells were acquired on a CyTOF instrument.

Data were normalized and analyzed using established pipelines. Immune cell populations were identified and characterized based on canonical marker expression, enabling comprehensive profiling of lymphoid and myeloid compartments within the bone marrow microenvironment.

Neutrophil culture and treatment

Mouse immature neutrophils (CD11b$^+$Ly6G$^+$CD101$^-$) were isolated from the bilateral femurs and tibias of Balb/c and C57BL/6 mice using FACS. The purified cells were cultured for 24 h with recombinant mouse DKK1 (50 ng/mL; Abcam, Cambridge, UK) and GM-CSF (50 ng/mL; PeproTech, Cranbury, NJ, USA). After incubation, the expression of maturation- and activation-associated markers, including Ly6G, CXCR2, CXCR4, and CD101, were assessed by flow cytometry on a Beckman CytoFLEX LX instrument (Beckman Coulter, Brea, CA, USA).

Neutrophil and CD8$^+$ T cell co-culture

Immature neutrophils were isolated and cultured as described above. CD8$^+$ T cells were obtained from the spleens of BALB/c and C57BL/6 mice using a CD8$^+$ T cell isolation kit (Miltenyi

Biotec, Bergisch Gladbach, Germany) and subsequently activated *ex vivo* as previously described[35]. After 3–5 d of activation, neutrophils and $CD8^+$ T cells were co-cultured in fresh medium at a 1:1 ratio (2×10^6 cells/mL each) for 48 h. Following co-culture, $CD8^+$ T cells were re-isolated using the same MACS-based method and the activation features and cytotoxic function were assessed as described in the subsequent sections.

Immunosuppression assays and cytotoxicity assay of $CD8^+$ T cells

After co-culture with neutrophils, $CD8^+$ T cells were collected and the activation status was evaluated by flow cytometry using antibodies against mouse CD25, CD69, and CD107a. Cytotoxicity was assessed by co-culturing $CD8^+$ T cells with tumor cells at an effector-to-target (E:T) ratio of 5:1, followed by CFSE/PI double staining (MedChemExpress, Monmouth Junction, NJ, USA) to evaluate cell viability, as previously described[35]. The percentage of apoptotic cells was calculated according to the following standard formula: $100 \times (PI^+ CFSE^+$ cells)/(total $CFSE^+$ cells) %. In addition, culture supernatants collected after the 8 h co-incubation were used for cytokine measurement, as described below.

Osteoclast induction

Bone marrow isolated from the femurs and tibias of BALB/c mice was flushed with cold DMEM (Gibco) and made into a red blood cell-free single-cell suspension. Cells were cultured with M-CSF and RANKL (R&D Systems, Minneapolis, MN, USA) to induce osteoclast precursor cells (OCPs), as described in a previous report[40]. After 7 d cells were treated with 50 ng/mL of recombinant mouse DKK1 or a mixture of DKK1 and 10 μg/mL of αDKK1 for an additional 48 h. Osteoclast-like cells were stained with a TRAP staining kit (Servicebio, Wuhan, China). $TRAP^+$ cell density (cells/mm) was quantified using Image-Pro Plus 6.0 (Media Cybernetics, Rockville, MD, USA). The identification of $TRAP^+$ multinucleated osteoclast-like cells was independently confirmed by an experienced pathologist based on morphologic criteria (≥3 nuclei and strong TRAP staining).

Macrophage induction

Bone marrow cells were harvested from the bilateral femurs and tibias of BALB/c and C57BL/6 mice, collected by centrifugation, and seeded into 12-well plates at a density of 1×10^6 cells/mL in medium supplemented with 10% FBS (Gibco) and 50 ng/mL of M-CSF (PeproTech). The medium was refreshed on day 3 and macrophage differentiation was confirmed by flow cytometry on day 5.

Ex vivo mouse macrophage polarization and treatment

Bone marrow-derived macrophages (BMDMs) from BALB/c or C57BL/6 mice were seeded at 3×10^5 cells per well in 12-well plates. Cells were left untreated as controls or polarized to an M1 phenotype with LPS (50 ng/mL; Sigma-Aldrich) for 48 h. Cells in separate groups were pre-incubated with recombinant mouse DKK1 (50 ng/mL), DKK1 + αDKK1 (10 μg/mL), or DKK1 + αCKAP4 [10 μg/mL (3F11-2B10, provided by Professor Akira Kikuchi from Osaka University, Osaka Prefecture, Japan)] for 48 h. After stimulation, cells were harvested and washed with PBS. Flow cytometry was performed to detect surface markers (CD45, CD11b, F4/80, CD80, CD86, and CD163) and intracellular markers (CD206, iNOS, and Arg1), as described above.

Ex vivo mouse myeloid cell culture and polarization

One week after tumor inoculation, $CD11b^+$ myeloid cells were isolated from the bone marrow of 4T1 bone metastasis-bearing BALB/c mice using anti-mouse CD11b magnetic beads (Miltenyi Biotec, Bergisch Gladbach, Germany). Purified $CD11b^+$ cells were seeded in 12-well plates at a density of 5×10^5 cells per well in RPMI-1640 complete medium. Cells were then stimulated with lipopolysaccharide [LPS] (50 ng/mL; Sigma-Aldrich) alone or in combination with recombinant mouse DKK1 (50 ng/mL; Abcam), DKK1 + αDKK1 [10 μg/mL; provided by (Leap Therapeutics, Cambridge, MA, USA)], or DKK1 + αCKAP4 [10 μg/mL, (3F11-2B10, provided by Professor Akira Kikuchi from Osaka University, Osaka Prefecture, Japan)] for 48 h at 37°C in a 5% CO_2 incubator. After stimulation, cells were harvested and washed twice with PBS. Flow cytometry was performed to detect surface markers (CD45, CD11b, F4/80, CD80, CD86, CD163, Ly6G, CD101, and CD61) and intracellular markers (CD206), as described above.

Cytometric bead array (CBA) analysis

The concentrations of IFN-γ, IL-6, TNF-α, CCL2, and IL-10 in cell culture supernatants were measured using the CBA Mouse IFN-γ Flex Set and the CBA Mouse Inflammation Kit (BD Biosciences). Sample acquisition was performed on a flow cytometer (Beckman CytoFLEX LX).

Statistical analysis

All statistical analyses and data visualization were performed using GraphPad Prism 10 (GraphPad Software, San Diego, CA, USA). The two-tailed Student's *t*-test was applied for two-group comparisons. One-way ANOVA was used for comparisons among three or more groups. All values are shown as the mean ± SEM. Statistical significance was set at a $P < 0.05$. Significance is denoted as ns (not significant), $^*P < 0.05$, $^{**}P < 0.01$, $^{***}P < 0.001$, and $^{****}P < 0.0001$.

Results

The bone metastasis microenvironment is predominantly composed of immunosuppressive myeloid cell populations

A 4T1 syngeneic bone metastasis model was established using the previously reported intra-caudal artery (CA) injection method to determine the immune landscape of the bone

metastasis microenvironment[41]. Bone marrow samples were harvested from tumor-free and bone metastasis-bearing mice, and $CD45^+$ immune cells were isolated for high-dimensional immune profiling using CyTOF. Unbiased hierarchical clustering combined with supervised annotation identified 26 distinct immune cell populations, including monocytes/macrophages (Mono/Mac), neutrophils, DCs, eosinophils, basophils, B cells, $CD4^+$ T cells, $CD8^+$ T cells, and NK cells (**Figure 1A–C**). Bone metastasis-bearing mice exhibited a markedly altered bone marrow immune landscape that was characterized by prominent expansion of myeloid subsets, particularly Mono/Mac and neutrophils, together with a notable reduction in DCs compared to tumor-free mice (**Figure 1D**). In addition, the frequencies of effector lymphocyte populations, including B cells, $CD4^+$ T cells, $CD8^+$ T cells, and NK cells, were significantly decreased in the bone metastasis group (**Figure 1E**). Interestingly, eosinophils were markedly enriched in the bone marrow of metastatic mice, whereas basophil frequencies remained unchanged (**Figure 1E**), indicating a specific remodeling of granulocyte populations during bone metastatic progression.

Zoledronic acid, a standard treatment for patients with bone metastases, was administered once each week to 4T1 bone metastasis-bearing mice and the tumor burden and immune alterations within the bone TME were evaluated (**Figure 1F**). Direct observation and micro-MRI demonstrated that zoledronic acid treatment failed to suppress bone metastasis growth (**Figure 1G, H**). Flow cytometry analysis of the bone marrow immune microenvironment showed no significant changes in the abundance of $CD8^+$ T cells, NK cells, or DCs following treatment (**Figure 1I–K**). Although the total proportion of macrophages was not significantly changed, zoledronic acid treatment significantly promoted a phenotypic shift toward an M1-like state (**Figure 1L, M**), indicating partial alleviation of the immunosuppressive macrophage phenotype. However, neutrophil frequency and maturation status remained unchanged after treatment (**Figure 1N**), suggesting that zoledronic acid alone provides only limited modulation of the myeloid compartment, which is insufficient to elicit an antitumor response in bone metastases.

DKK1 impairs neutrophil maturation to induce immunosuppressive function

Given the pivotal roles of myeloid cells, including neutrophils, osteoclasts, and macrophages within the bone TME, elucidating the regulatory mechanisms underlying cellular differentiation and function is essential for developing effective therapies. In our recent study we identified a significant upregulation of DKK1 in bone metastases compared to primary tumors[21], suggesting a potential role in shaping the immunosuppressive bone metastasis microenvironment. To further define how DKK1 signaling influences the phenotype and function of these key myeloid subsets, a series of comprehensive *ex vivo* functional assays were performed. Immature neutrophils have been increasingly recognized as key mediators of immunosuppression within the TME. Given the numerical abundance and immunoregulatory potential in the bone marrow, we sought to investigate whether DKK1 contributes to immune evasion by modulating neutrophil maturation. Immature neutrophils ($Ly6G^+CD101^-$) were first isolated from the bone marrow of healthy C57BL/6 mice by flow cytometry and subjected to *ex vivo* differentiation assays. Upon GM-CSF stimulation, these neutrophils progressively acquired phenotypic markers of maturation, including upregulation of Ly6G, CXCR2, and CD101, along with downregulation of CXCR4 (**Figure 2A**). However, the addition of recombinant mouse DKK1 protein significantly impaired GM-CSF-induced neutrophil maturation (**Figure 2A**), indicating that DKK1 has a crucial role in maintaining the immature state of neutrophils.

To evaluate the immunological consequences of this impaired maturation, flow-sorted immature neutrophils were treated with GM-CSF alone or in combination with DKK1 for 24 h followed by co-culture with magnetically isolated splenic $CD8^+$ T cells (**Figure 2B**). Functional assays revealed that immature neutrophils profoundly suppress $CD8^+$ T-cell activation, while GM-CSF-induced maturation markedly attenuates the immunosuppressive capacity (**Figure 2C–E**). Notably, DKK1 exposure restored the immunosuppressive phenotype of these neutrophils, as evidenced by decreased IFN-γ production (**Figure 2C**), reduced expression of $CD8^+$ T-cell activation markers [CD25, CD69, and CD107a] (**Figure 2D**), and impaired cytotoxicity against LLC tumor cells (**Figure 2E**). Collectively, these findings identified DKK1 as a critical regulator of neutrophil maturation, sustaining an immunosuppressive state of immature neutrophils that compromises $CD8^+$ T-cell effector functions *ex vivo*.

Neutrophil-specific Ckap4 deletion promotes neutrophil maturation and restrains bone metastatic tumor progression

CKAP4 is a transmembrane receptor that was recently identified as a functional binding partner of DKK1[27]. CKAP4 transduces downstream signaling that regulates cellular functions, such as proliferation, differentiation, and immune modulation by directly interacting with DKK1. This finding suggests that binding of DKK1 to CKAP4 on TANs may impair neutrophil maturation and alter the functional properties, which contributes to tumor-promoting effects (**Figure 3A**). Neutrophil-specific *Ckap4* knockout mice ($Ckap4^{fl/fl}S100a8^{Cre}$) were generated to further elucidate the role of CKAP4 in regulating neutrophil

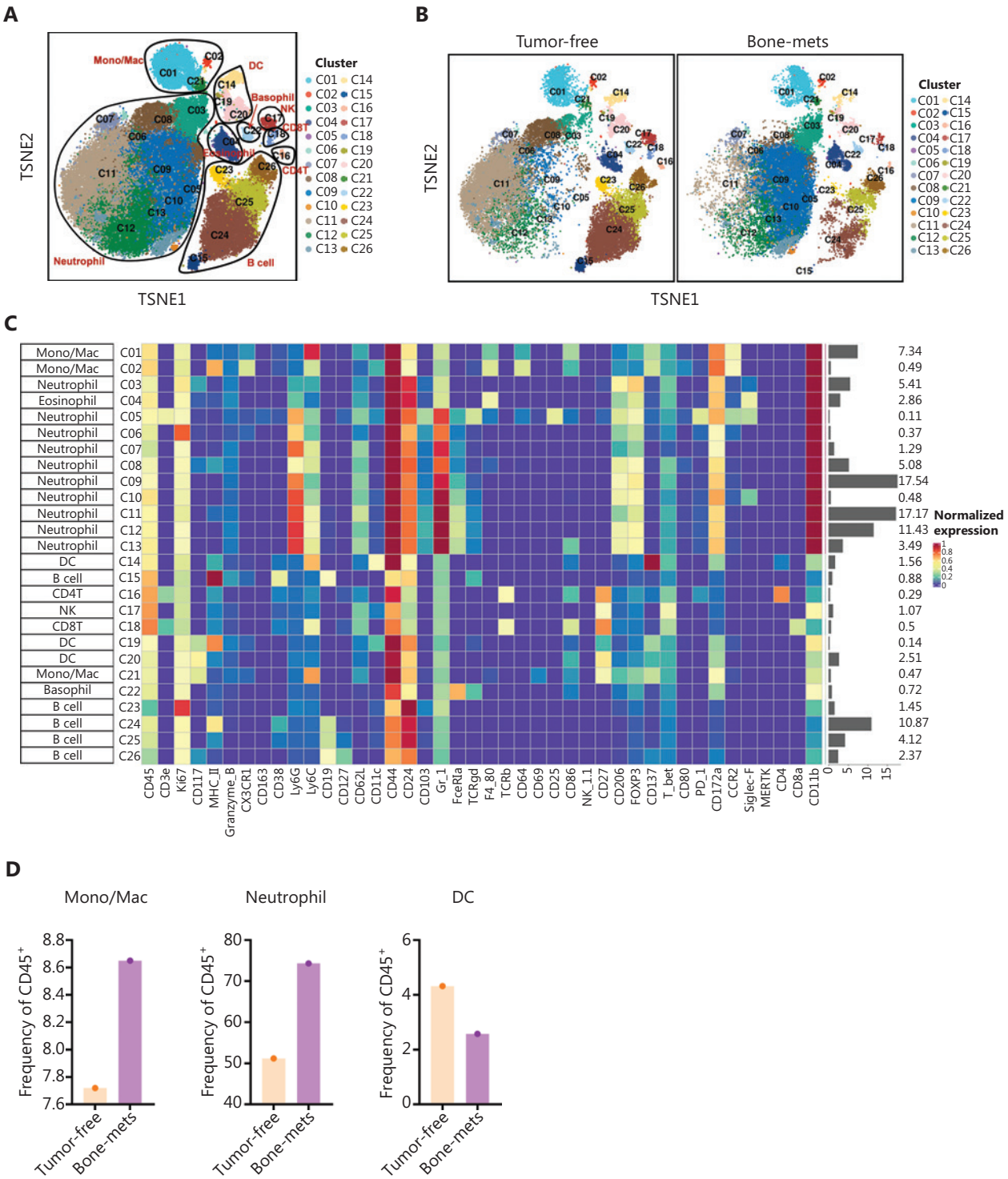


Figure 1 Continued

maturation and the impact on tumor progression (**Figures 3B and S1**). This model enables neutrophil-specific gene deletion with high efficiency and minimal off-target recombination in other myeloid compartments. Bone metastasis models were established by CA injection of LLC cells into a *Ckap4*$^{fl/fl}$ and *Ckap4*$^{fl/fl}$*S100a8*^{Cre} mouse model

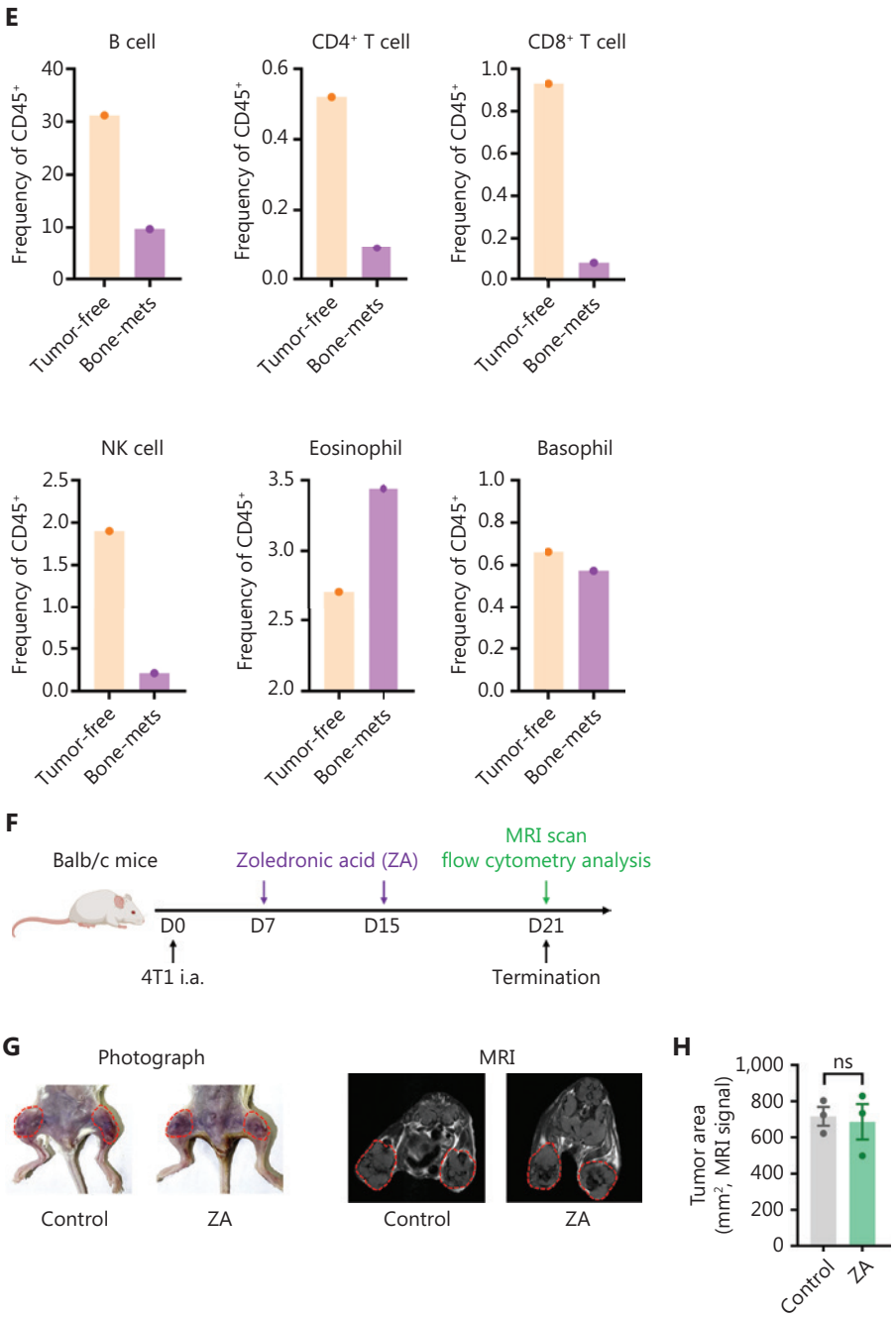


Figure 1 Continued

with experimental endpoints set at day 28. Direct observation and micro-MRI imaging revealed that deletion of *Ckap4* in neutrophils significantly suppresses bone metastatic tumor growth compared to the *Ckap4*$^{fl/fl}$ control group (**Figure 3C, D**).

Bone marrow samples were harvested to investigate changes in the bone metastasis microenvironment at the endpoint for analysis. Flow cytometry confirmed enhanced neutrophil maturation in the bone marrow of *Ckap4*$^{fl/fl}$*S100a8*^{Cre} mice (**Figure 3E**). Analysis of myeloid cells revealed a substantial increase in M1-like macrophages (CD86$^+$F4/80$^+$), a reduction in M2-like macrophages (CD163$^+$F4/80$^+$), and increased activation of DCs (**Figure 3F, G**). Importantly, both the frequency and activation status of CD8$^+$ T cells were significantly elevated in *Ckap4*-deficient mice compared to controls (**Figure 3H, I**). Collectively, these results demonstrated that CKAP4 acts as

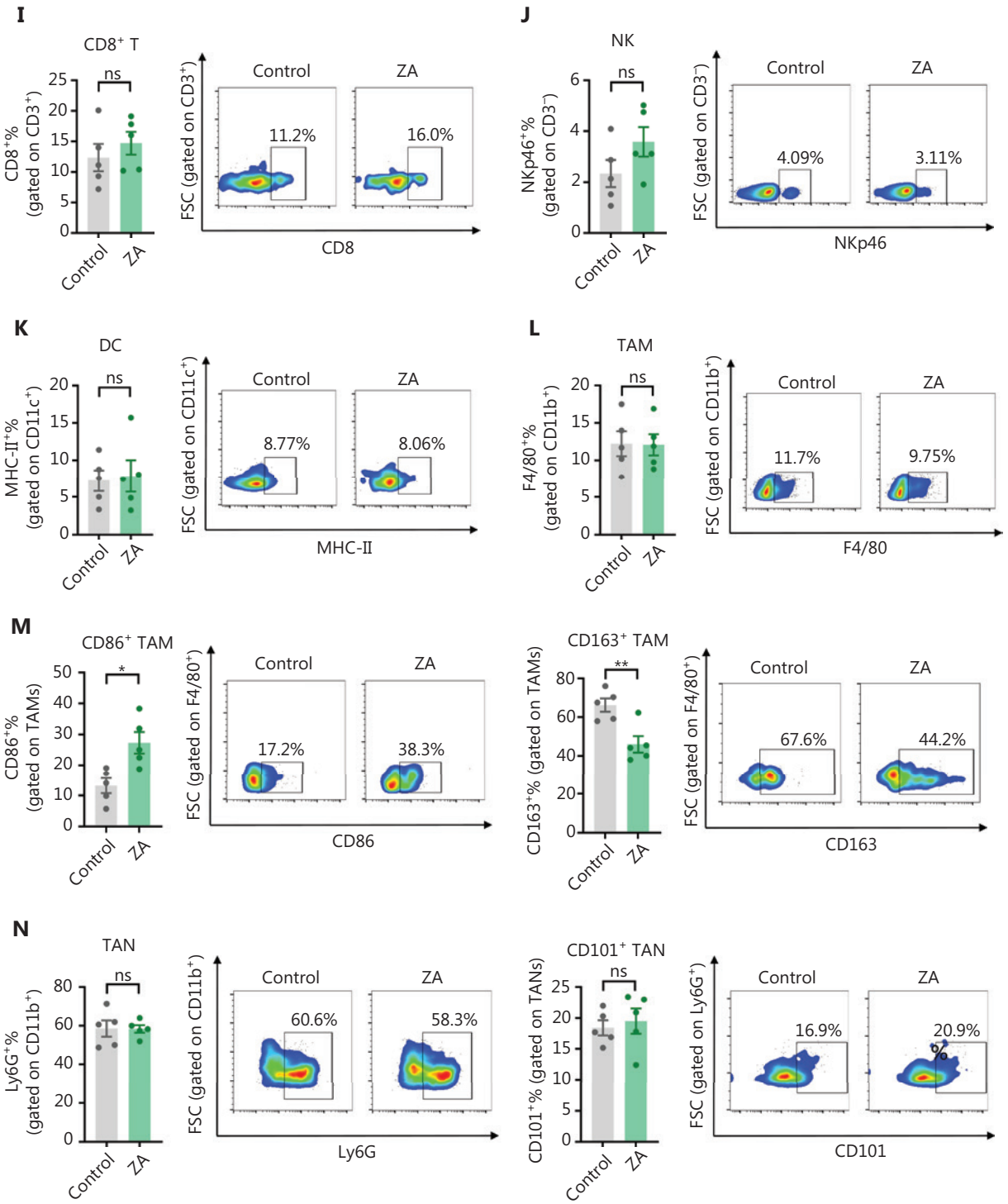


Figure 1 The bone metastasis microenvironment is predominantly composed of immunosuppressive myeloid cell populations. (A) t-SNE analysis of immune cell populations from bone marrow of tumor-free mice (tumor-free) and mice with established bone metastases (bone-mets), identifying distinct cell clusters (C01-C26). (B) t-SNE plots showing the distribution of immune cell clusters in the bone marrow from tumor-free mice and bone-mets mice. (C) Heatmap displaying the differential expression of selected marker across the identified immune cell clusters. (D, E) Quantification of the frequency of major immune cells in the bone marrow of tumor-free mice and bone-mets mice: (D) Monocytes/macrophages, neutrophils, and DCs; (E) B cells, $CD4^+$ T cells, $CD8^+$ T cells, NK cells, eosinophils, and basophils. (F) Schematic of the 4T1 bone metastasis model establishment and treatment (zoledronic acid, 100 μg/kg, i.p., 2 doses over 21 days). (G) Representative

images and MRI scans of bone metastases at day 21. (H) Quantification of tumor burden. (I–N) Flow cytometry analysis of bone metastasis microenvironment for: (I) $CD8^+/CD3^+$ T cells; (J) $NKp46^+/CD45^+$ $CD3^-$ NK cells; (K) $MHC\text{-}II^+/CD11c^+$ dendritic cells; (L) $F4/80^+/CD11b^+$ macrophages; (M) $CD86^+$ and $CD163^+$ macrophages; (N) $Ly6G^+/CD11b^+$ cells and $CD101^+$ TANs. Bone-mets, bone-metastases; DC, dendritic cell; i.a., intraarterial; Mac, macrophage; Mono, monocyte; MRI, magnetic resonance imaging; NK, natural killer; TAM, tumor-associated macrophage; TAN, tumor-associated neutrophil; ZA, zoledronic acid. Significance is denoted as ns (not significant), $*P < 0.05$, and $**P < 0.01$.

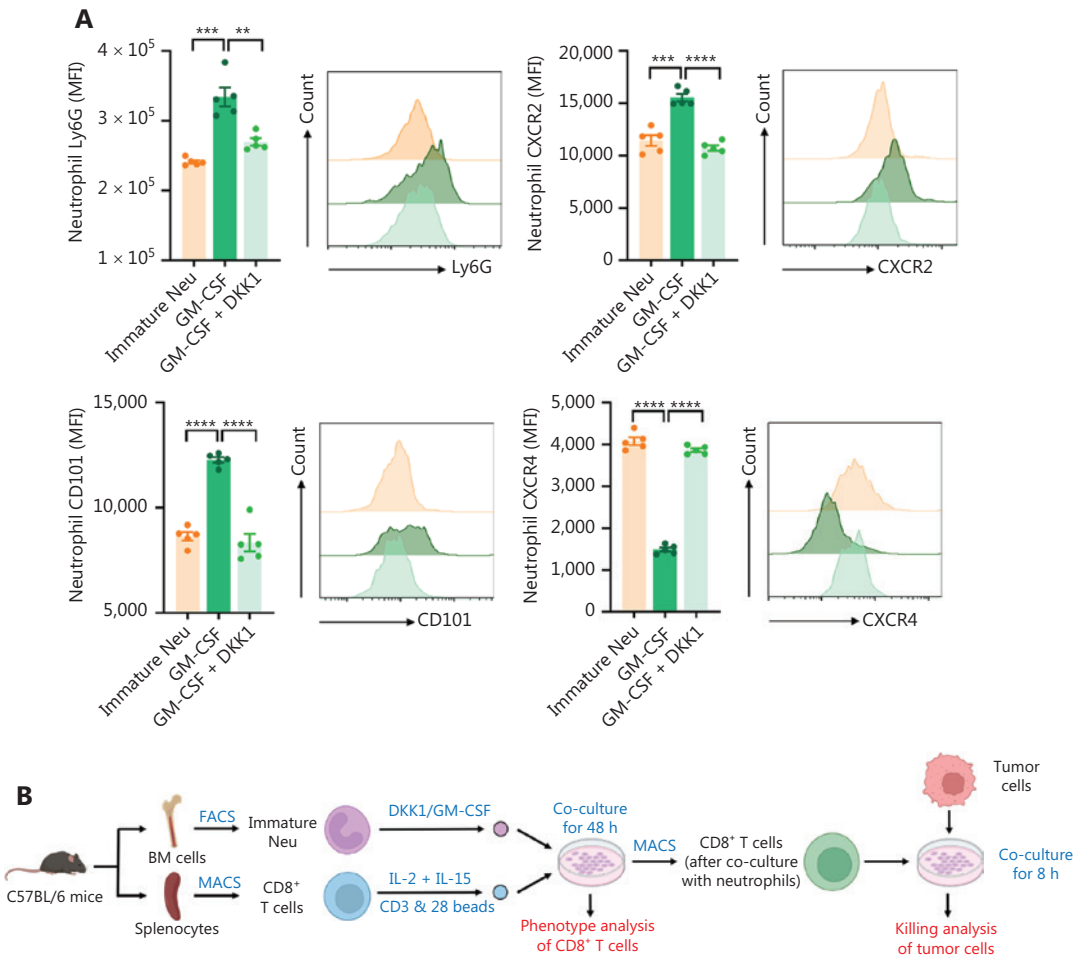


Figure 2 Continued

a key receptor mediating the immunosuppressive effects of DKK1 on neutrophil maturation. Inhibition of DKK1-CKAP4 signaling in neutrophils restores maturation and remodels the immunosuppressive microenvironment, thereby enhancing antitumor immune responses and restraining bone metastatic tumor progression.

DKK1 promotes the differentiation of OCPs into osteoclast-like cells

Bone marrow cells from healthy mice were induced into OCPs *ex vivo* with M-CSF and RANKL stimulation to investigate the regulatory role of DKK1 in osteoclast differentiation (**Figure 4A**). After 7 days of induction recombinant DKK1 protein or DKK1 combined with αDKK1 was added for an additional 48 h co-culture. TRAP staining confirmed that DKK1 stimulation significantly increased the number of $TRAP^+$ multinucleated osteoclast-like cells, while the addition of αDKK1 markedly attenuated this increase (**Figure 4B, C**), suggesting that DKK1 may promote the differentiation of OCPs toward an osteoclast-like phenotype. Furthermore, the functional activity of these osteoclast-like cells was evaluated by measuring the secretion of inflammatory cytokines, including IL-6, CCL2, and TNF-α. Osteoclast-like cells exhibited

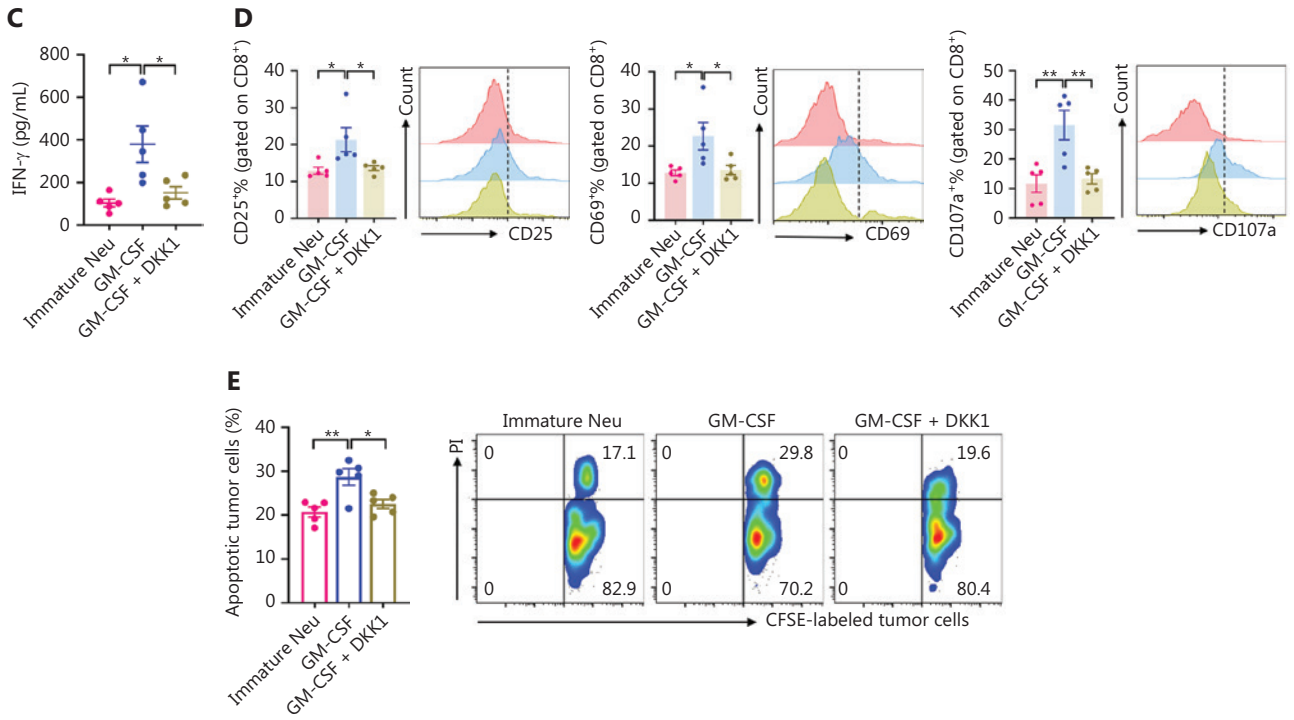


Figure 2 DKK1 induces immature and immunosuppressive TANs in bone metastases. (A) Immature neutrophils sorted from mouse bone marrow were stimulated *ex vivo* with GM-CSF (50 ng/mL) or GM-CSF + DKK1 (50 ng/mL); mean fluorescence intensity (MFI) of Ly6G, CXCR2, CD101, and CXCR4 were assessed by flow cytometry. (B) Sorted immature neutrophils were treated with or without GM-CSF and DKK1 for 24 h, then co-cultured with primary $CD8^+$ T cells (1:1) for 48 h. (C) The IFN-γ secretion was measured after co-culture. (D) CD25, CD69, and CD107a expression in $CD8^+$ T cells were analyzed by flow cytometry. (E) After co-culture, $CD8^+$ T cells were further co-cultured with CFSE-labeled tumor cells at a 5:1 ratio and tumor cell apoptosis was measured after 8 h. BM, bone marrow; DKK1, dickkopf-1; GM-CSF, granulocyte-macrophage colony-stimulating factor; MACS, magnetic activated cell sorting; Neu, neutrophil. Significance is denoted as ns (not significant), $^*P < 0.05$, $^{**}P < 0.01$, $^{***}P < 0.001$, and $^{****}P < 0.0001$.

enhanced proinflammatory cytokine production following DKK1 co-culture, whereas the addition of αDKK1 significantly attenuated this effect (**Figure 4D**). These findings suggested that DKK1 enhances proinflammatory activity, which may further contribute to the immunosuppressive and osteolytic features of the tumor-bone microenvironment in addition to promoting differentiation of OCPs into osteoclast-like cells.

GSEA was performed to validate these results in clinical datasets using transcriptomic datasets from patients with breast cancer (GSE14018, GSE14020, and GSE54323). The results revealed a significant positive correlation between DKK1 expression and osteoclast-related gene signatures, including pathways related to osteoclast differentiation, bone resorption, osteopenia, and cancer-related bone pain. Conversely, DKK1 expression was negatively correlated with osteoblast differentiation, ossification, bone remodeling, and BMP signaling pathways (**Figure 4E**). Collectively, these results support a role for DKK1 in promoting osteoclast-like differentiation and inflammatory activity, thereby potentially contributing to osteolytic bone destruction.

DKK1 promotes M2-like polarization and immunosuppressive function of macrophages

Macrophage polarization and functional status have important roles in tumor initiation and progression[42,43]. *Ex vivo* stimulation assays were performed to further explore the role of DKK1 in macrophage polarization using BMDMs. Bone marrow cells isolated from healthy BALB/c and C57BL/6 mice were cultured with M-CSF for 5 d to generate M0 macrophages. These cells were then stimulated with LPS to induce classical M1 polarization, then treated with recombinant DKK1 protein, DKK1 plus αDKK1, or DKK1 plus αCKAP4 (**Figure 5A, E**). Cytokine production by macrophages was first examined under different stimulation conditions. Stimulation with recombinant DKK1 protein in BALB/c-derived BMDMs led to significant upregulation of the immunosuppressive chemokine, CCL2, while this effect was markedly reversed upon co-treatment with αDKK1 (**Figure 5B**). DKK1 stimulation in C57BL/6-derived BMDMs resulted in a notable reduction in pro-inflammatory cytokines (IL-6 and TNF-α) accompanied by increased secretion of CCL2 and the anti-inflammatory

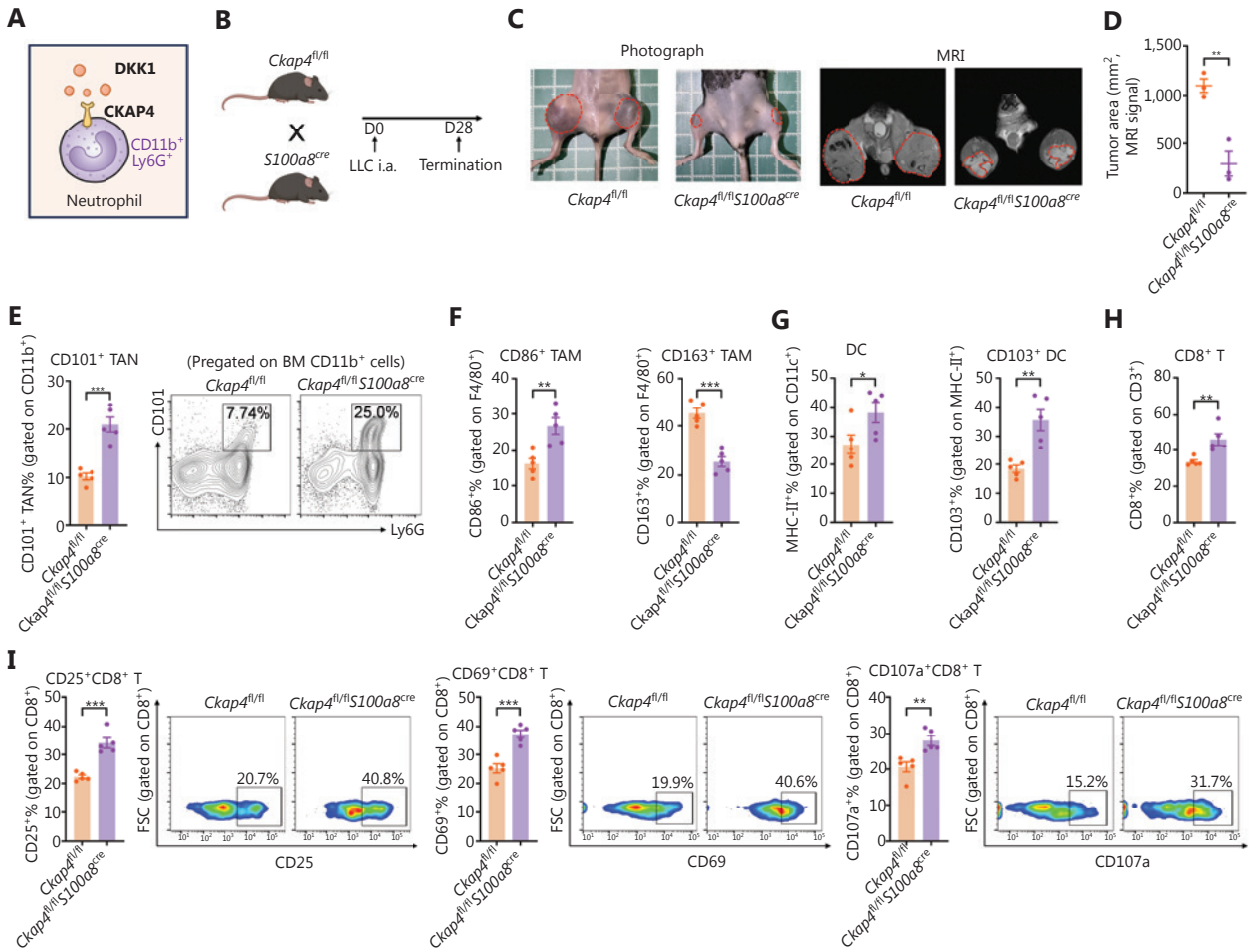


Figure 3 Neutrophil-specific *Ckap4* deletion promotes neutrophil maturation and restrains bone metastases tumor progression. (A) Schematic illustrating DKK1-CKAP4 interaction on neutrophils. (B, C) *Ckap4*$^{fl/fl}$ and *Ckap4*$^{fl/fl}$*S100a8*^{cre} mice were injected intra-arterially with LLC cells. Representative endpoint images and MRI scans of bone metastases are shown. (D) Quantification of tumor burden. (E) Proportion of mature neutrophils (CD11b$^+$Ly6G$^+$CD101$^+$) in bone marrow analyzed by flow cytometry. (F–I) Flow cytometry analysis of bone TME for (F) CD86$^+$/F4/80$^+$, CD163$^+$/F4/80$^+$; (G) MHC-II$^+$/CD11c$^+$, CD103$^+$ DCs; (H) CD8$^+$/CD3$^+$ T cells; (I) CD25$^+$/CD8$^+$, CD69$^+$/CD8$^+$, and CD107a$^+$/CD8$^+$ cells. BM, bone marrow; CKAP4, cytoskeleton-associated protein 4; DC, dendritic cell; DKK1, dickkopf-1; MRI, magnetic resonance imaging; TAM, tumor-associated macrophage; TAN, tumor-associated neutrophil. Data are presented as mean ± SEM. ns, not significant, **P* < 0.05, ***P* < 0.01, and ****P* < 0.001.

cytokine, IL-10 (**Figure 5F**). Again, these effects were effectively reversed by DKK1 blockade with αDKK1, which restored a pro-inflammatory cytokine profile (**Figure 5B, F**).

Consistent with these cytokine profiles, flow cytometric analysis revealed that recombinant DKK1 protein markedly suppressed LPS-induced M1 polarization, as evidenced by a reduced percentage of CD80$^+$CD86$^+$ macrophages (**Figure 5C, G**). Conversely, DKK1 concurrently promoted the expression of M2-associated markers, reflected by an increased proportion of CD163$^+$CD206$^+$ macrophages (**Figure 5D, H**), indicating that DKK1 skews macrophage polarization toward an immunosuppressive M2-like phenotype. Co-treatment with αDKK1 or αCKAP4 partially reversed the suppressive effects of DKK1, restoring M1-associated marker expression and reducing the acquisition of M2 features (**Figure 5C, D, G, H**). In support of these experimental findings, integrative transcriptomic analyses of human breast cancer databases (GSE14018, GSE14020, and GSE54323) showed that DKK1 expression is positively correlated with myeloid-derived chemokines, such as CCL20, CCL7, and CXCL5, as well as pro-tumor neutrophil markers, like S100A8 and S100A9 (**Figure 5I**). In parallel, DKK1 expression negatively correlated with TNFRSF14, a known co-stimulatory molecule involved in T-cell activation (**Figure 5I**). Together, these results indicated that DKK1 promotes macrophage-mediated immunosuppression by skewing macrophage polarization toward the M2 phenotype, thereby fostering the formation of an immunosuppressive TME conducive to tumor progression.

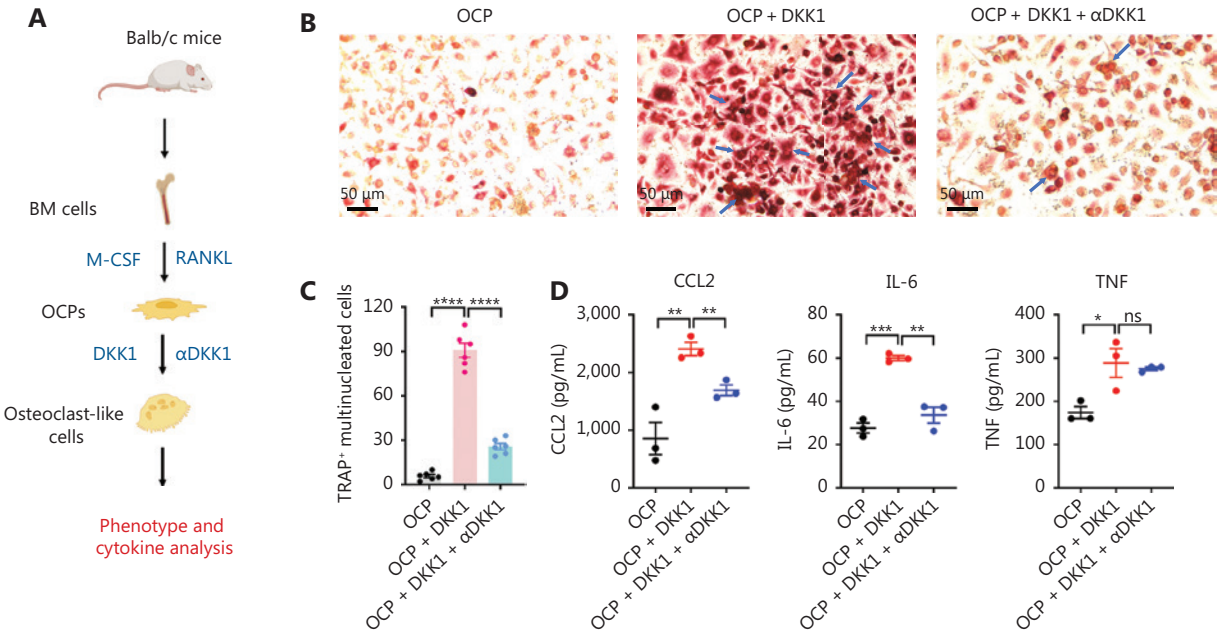


Figure 4 Continued

The DKK1-CKAP4 axis globally reprograms multiple myeloid cell populations in the bone metastasis microenvironment

A 4T1 bone metastasis model was established to investigate the impact of the DKK1-CKAP4 axis on global myeloid cell populations within the bone metastasis microenvironment. $CD11b^+$ myeloid cells were isolated from the bone marrow 7 d after tumor inoculation and cultured *ex vivo* in the presence of LPS with or without recombinant DKK1 protein, αDKK1, or αCKAP4 (**Figure S2A**). After 48 h flow cytometric analysis revealed that co-culture with DKK1 significantly reduced CD101 expression on neutrophils (**Figure S2B**), increased the proportion of $CD61^+$ osteoclast-like cells (**Figure S2C**), decreased the frequency of $CD80^+CD86^+$ M1-like macrophages (**Figure S2D**), and elevated the percentage of $CD163^+CD206^+$ M2-like macrophages (**Figure S2E**). Conversely, co-treatment of αDKK1 or αCKAP4 restored CD101 expression on neutrophils, reduced the proportion of $CD61^+$ osteoclast-like cells, increased M1-like macrophages, and decreased M2-like macrophages (**Figure S2B–E**). Of note, CD61 has been reported to be expressed not only on osteoclasts but also on megakaryocytes and platelets[44,45]. In our study $CD11b^+$ myeloid cells were positively selected prior to differentiation, which effectively excluded megakaryocytes and platelets. Therefore, an increase in CD61 expression may indicate enhanced differentiation of OCPs toward an osteoclast-like phenotype. These findings indicated that DKK1, acting through CKAP4, globally reprograms multiple myeloid lineages toward an immunosuppressive phenotype. Blockade of DKK1-CKAP4 signaling effectively reverses this myeloid-suppressive program.

Single-cell RNA sequencing data from the GSE143791 dataset were analyzed to investigate the role of the DKK1-CKAP4 pathway in the human bone metastatic tumor microenvironment, which includes samples from bone metastatic prostate tumors (tumor site), uninvolved bone marrow (distal), and bone marrow from cancer-free orthopedic patients (benign). Dimensionality reduction and clustering using t-SNE were performed to visualize immune cell populations (**Figure S3A, B**). *CKAP4* expression was then examined across different immune cell subsets, which showed that *CKAP4* was predominantly expressed in myeloid cells (**Figure S3C**). Analysis of *CKAP4* expression levels in myeloid cells across the different sample groups revealed that *CKAP4* was primarily expressed in the tumor site group (**Figure S3D**). Myeloid cells in the tumor site were stratified into *CKAP4*-high and -low subgroups based on *CKAP4* expression. Comparison of gene signatures between the two subgroups showed that the *CKAP4*-high subgroup exhibited elevated expression of immunosuppressive-related genes, including *LGALS9*, *LILRB3*, *LILRB2*, *HIF1A*, *CD44*, *CD47*, *PTPN2*, *TGIF1*, and *S100A8* (**Figure S3E**). In contrast, the *CKAP4*-low subgroup displayed higher expression of antigen-presentation-related genes, such as *HLA-DRA*, *HLA-DPB1*, *HLA-B*, *HLA-A*, *PSMB9*, *PSMB8*, *CTSS*, *CTSB*, and *CLEC7A* (**Figure S3F**). Collectively, these findings indicated that *CKAP4*-high myeloid cells possess a more immunosuppressive phenotype, while *CKAP4*-low myeloid cells exhibit

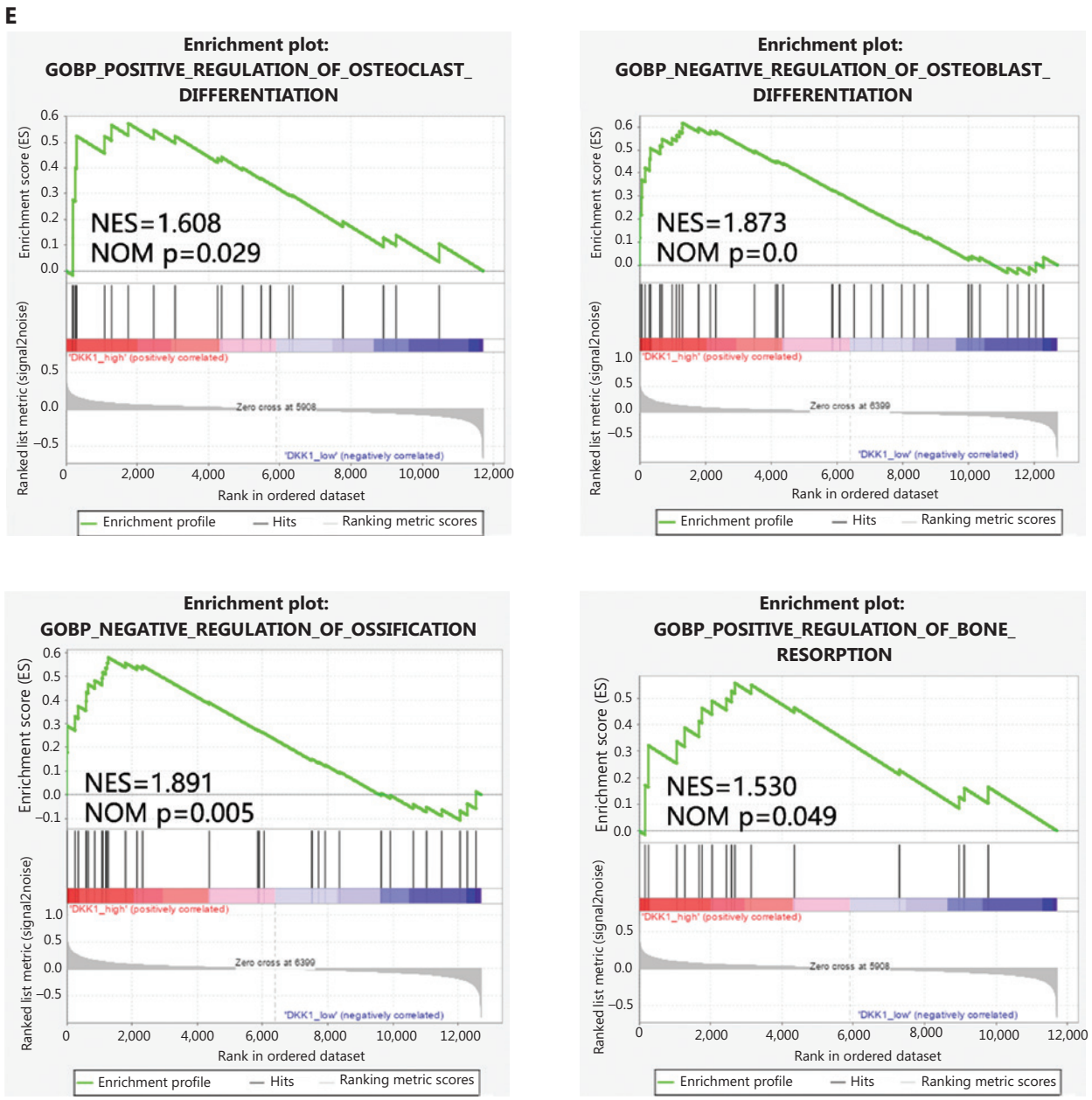


Figure 4 Continued

features consistent with immune activation and enhanced antigen presentation.

Combining myeloid cell reprogramming with zoledronic acid suppresses tumor progression and remodels the bone metastasis immune microenvironment

Given that DKK1 promotes osteoclast-like cell differentiation and the immunosuppressive functions of myeloid cells, we hypothesized that blockade of DKK1-CKAP4 signaling with αDKK1 in combination with zoledronic acid may exert potent antitumor effects. To test this hypothesis, a 4T1 bone metastasis model in BALB/c mice and an LLC bone metastasis model in C57BL/6 mice were separately established. Mice were treated with an αDKK1 or IgG2a isotype control intraperitoneally twice weekly, while zoledronic acid was administered intraperitoneally on days 7 and 15. The experimental endpoint was assessed on day 21 (**Figure 6A, D**). Direct observation and micro-MRI imaging demonstrated that αDKK1 treatment significantly suppressed tumor progression in both

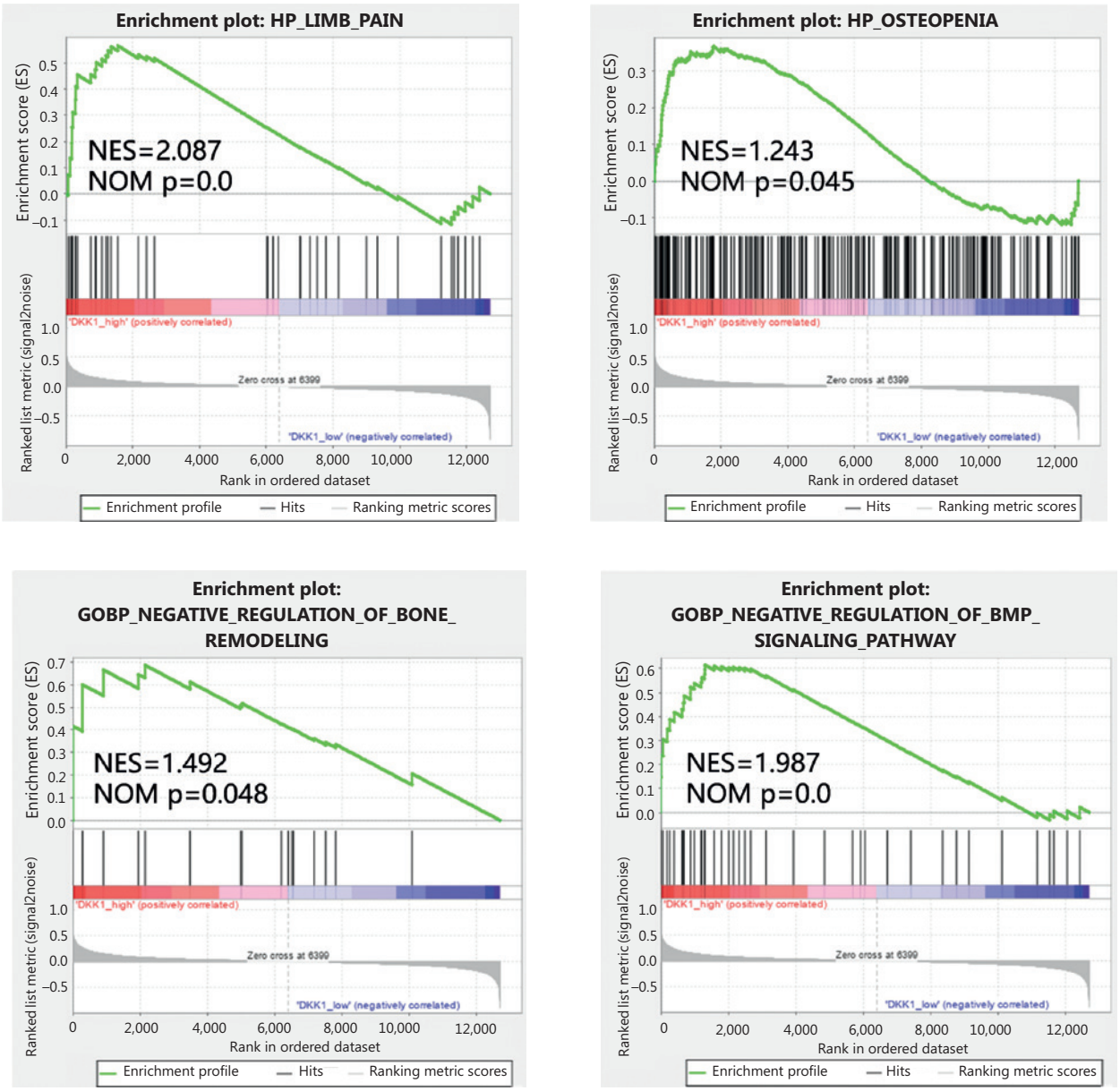


Figure 4 DKK1 promotes the maturation and activation of osteoclast progenitors. (A) Osteoclast precursor cells from Balb/c mouse bone marrow were differentiated *ex vivo* with M-CSF (50 ng/mL) and RANKL (50 ng/mL), then treated with DKK1 (50 ng/mL) or DKK1 plus αDKK1 (10 μg/mL). (B, C) TRAP staining was used to quantify $TRAP^+$ multinucleated cells with osteoclast-like features in each group. (D) Cytokines (IL-6, CCL2, and TNF-α) were measured after induction. (E) Gene set enrichment analysis (GSEA) of breast cancer GEO datasets (GSE14018, GSE14020, and GSE54323) showing the association between DKK1 expression and osteoclast- or osteoblast-related pathways. BM, bone marrow; DKK1, dickkopf-1; NES, normalized enrichment score; OCPs, osteoclast precursor cells; TRAP, tartrate-resistant acid phosphatase; αDKK1, DKK1 antibody. Significance is denoted as ns (not significant), $*P < 0.05$, $**P < 0.01$, $***P < 0.001$, and $****P < 0.0001$.

models without evident weight loss and the combination therapy produced a markedly greater reduction in tumor burden compared with αDKK1 monotherapy, supporting a synergistic antitumor effect (**Figures 6B, C, E, F and S4C, H**). H&E and TRAP staining was performed on bone metastasis sections in the 4T1 bone metastasis model. H&E staining confirmed that zoledronic acid alone failed to control bone metastatic progression, whereas αDKK1 treatment significantly reduced tumor infiltration with combination therapy showing much more pronounced effects. Moreover, zoledronic acid monotherapy decreased the number of osteoclasts and combination therapy led to a greater reduction (**Figure S4A, B**).

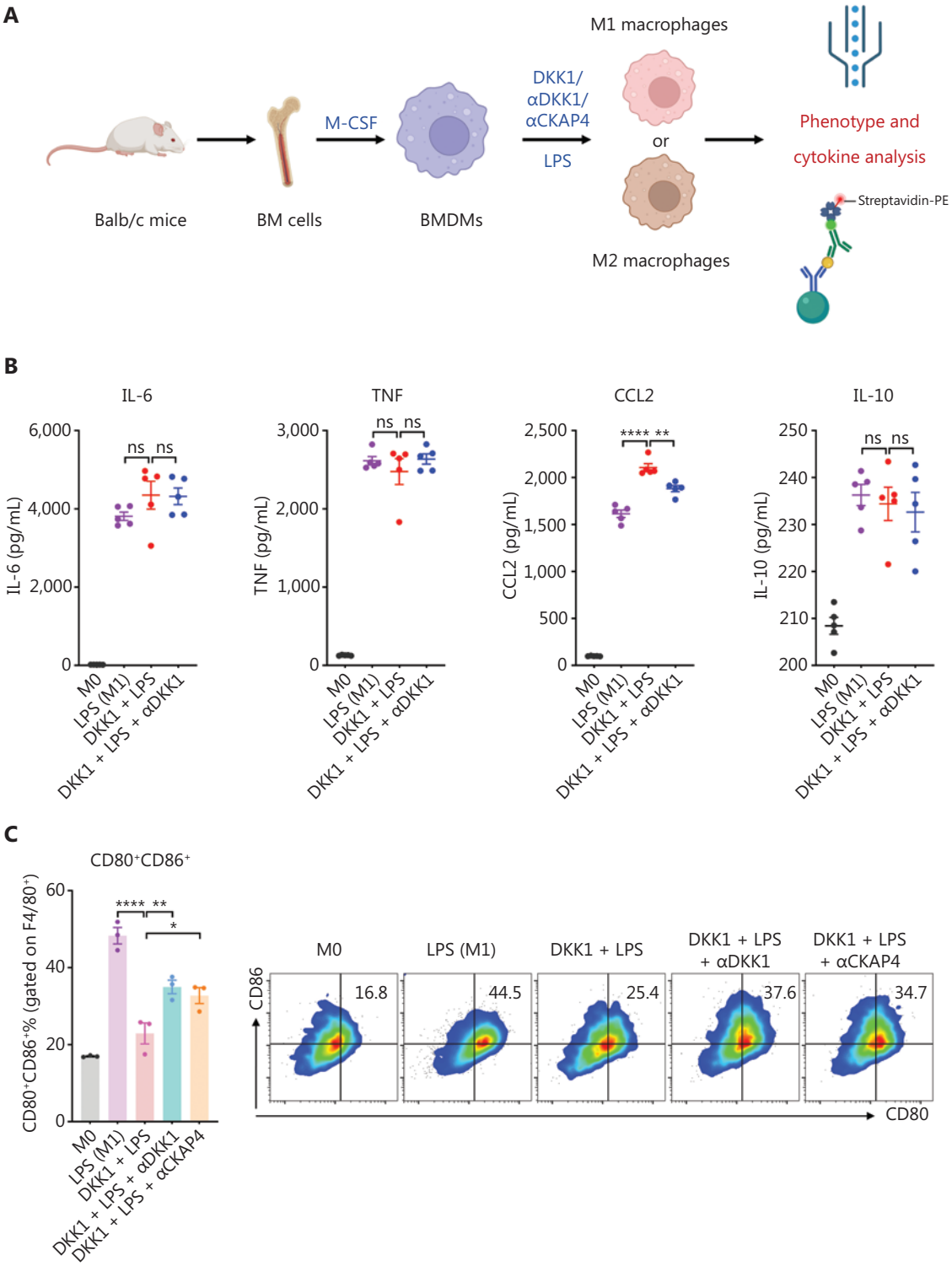


Figure 5 Continued

The composition and phenotypes of immune cells in the bone marrow of 4T1 and LLC bone metastases mice were analyzed to explore the alterations in immune competence within the bone TME following treatment (**Figures 6G–L and S4D–G, I–L**). DKK1 blockade alone substantially increased the frequency and activation of $CD8^+$ T cells (**Figure 6G, J**),

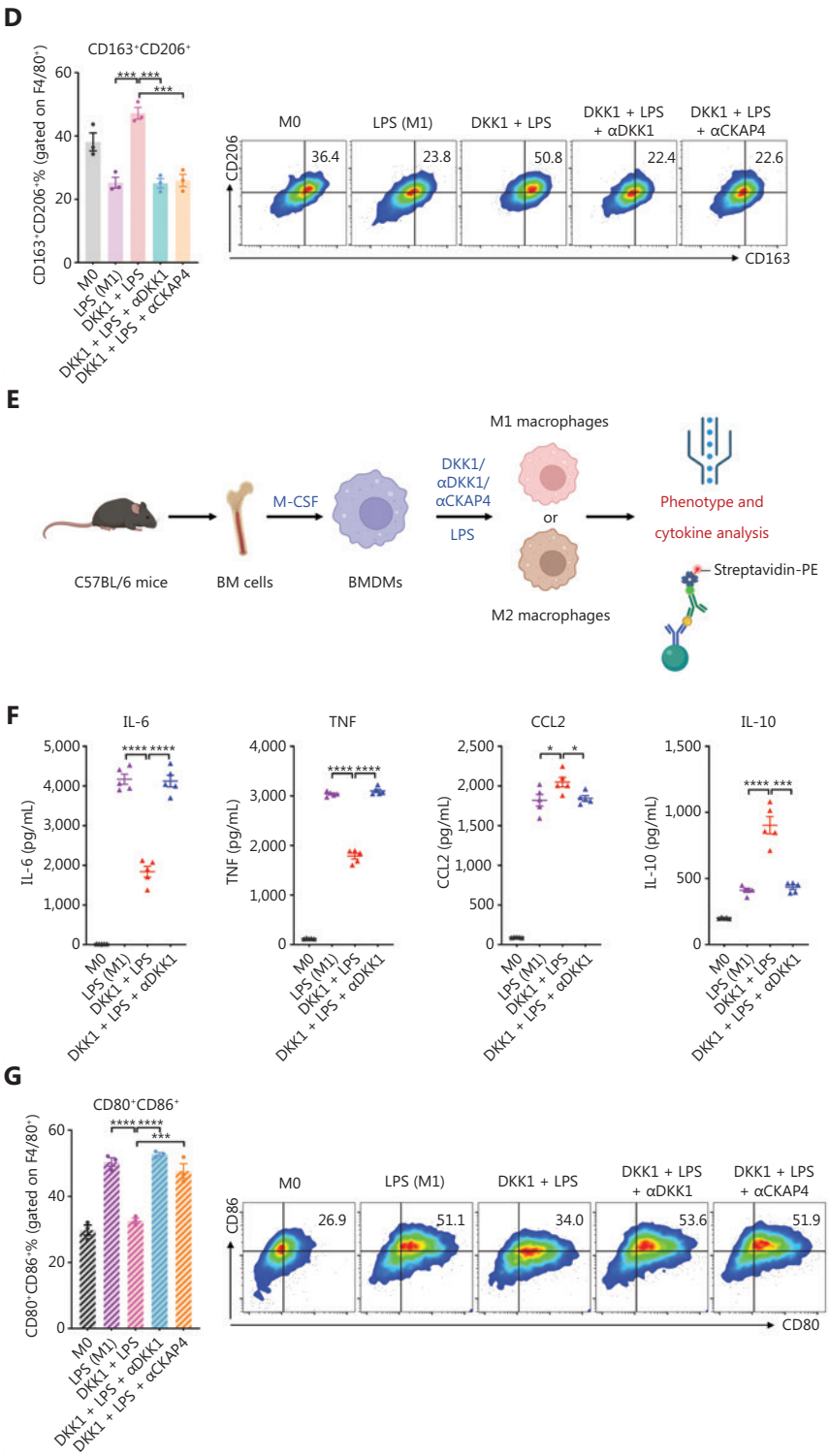


Figure 5 Continued

enhanced the infiltration of NK cells and MHC-II$^+$ DCs, and reduced the accumulation of Arg1$^+$ myeloid-derived suppressor cells [MDSCs] (**Figure S4D–F, I–K**). Although the overall frequency of Ly6G$^+$ neutrophils was not significantly altered, αDKK1 treatment promoted neutrophil maturation, as evidenced by increased expression of the maturation marker

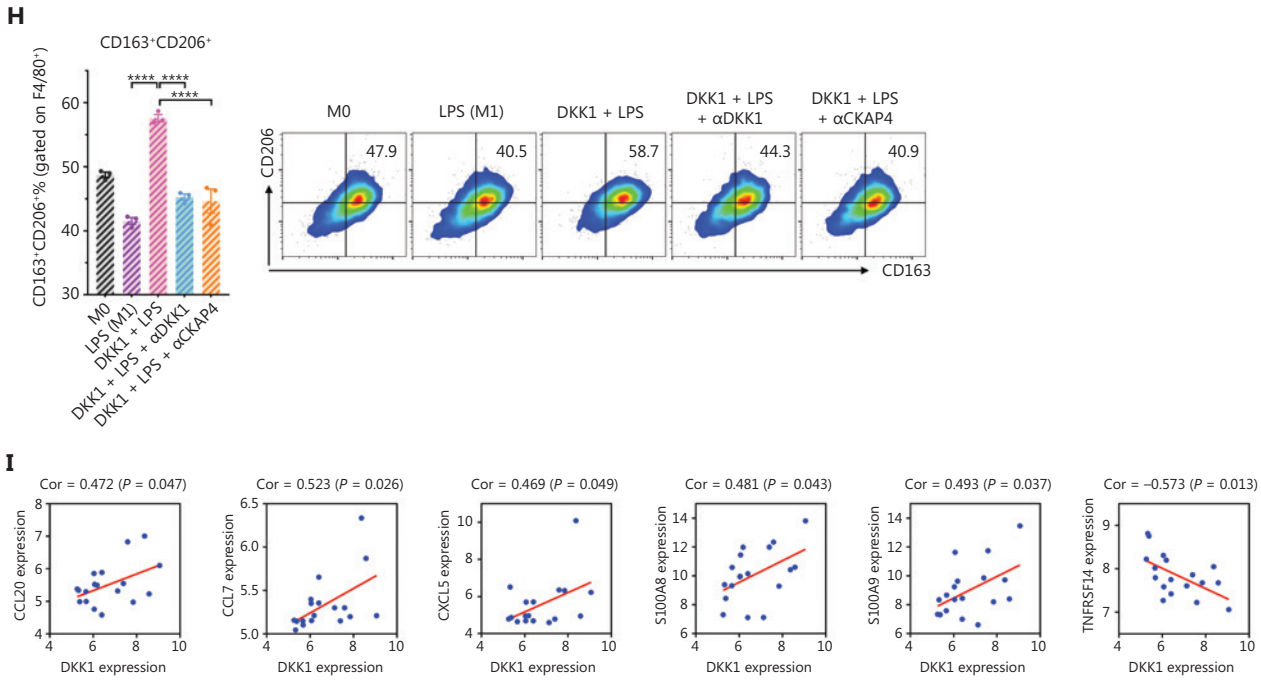


Figure 5 DKK1 induces M2 polarization and immunosuppressive function of macrophages. (A) BMDMs from Balb/c mice were stimulated with LPS (50 ng/mL) with or without DKK1 (50 ng/mL), αDKK1 (10 μg/mL), and αCKAP4 (10 μg/mL). After 48 h, (B) the concentrations of IL-6, TNF-α, CCL2, and IL10 in culture supernatants were detected by CBA. The proportion of (C) $CD80^+$ $CD86^+$ and (D) $CD163^+$ $CD206^+$ macrophages was determined by flow cytometry. (E) BMDMs from C57BL/6 mice were stimulated with LPS (50 ng/mL) with or without DKK1 (50 ng/mL), αDKK1 (10 μg/mL), and αCKAP4 (10 μg/mL). After 48 h, (F) the concentrations of IL-6, TNF-α, CCL2, and IL10 in culture supernatants were detected by CBA. The proportion of (G) $CD80^+$ $CD86^+$ and (H) $CD163^+$ $CD206^+$ macrophages was determined by flow cytometry. (I) Integrative transcriptomic analysis of human breast cancer GEO datasets (GSE14018, GSE14020, and GSE54323) showed correlations between DKK1 expression and myeloid-derived chemokines. BM, bone marrow; DKK1, Dickkopf-1; LPS, lipopolysaccharide; M-CSF, macrophage colony-stimulating factor; NES, normalized enrichment score; αCKAP4, CKAP4 antibody; αDKK1, DKK1 antibody. Significance is denoted as ns (not significant), $*P < 0.05$, $**P < 0.01$, $***P < 0.001$, and $****P < 0.0001$.

CD101 (**Figure 6H, K**). Moreover, DKK1 blockade reprogrammed macrophage polarization by increasing M1-like macrophages ($CD86^+$) and decreasing M2-like macrophages ($CD163^+$) (**Figures 6I, L and S4G, L**). Notably, administration of αDKK1 in healthy, tumor-free mice did not alter the composition or activation status of immune cell subsets in the bone marrow (**Figure S5**), indicating that the immunomodulatory effects are specific to the tumor-bearing context.

Combination treatment induced more pronounced microenvironment remodeling compared to DKK1 blockade alone. Specifically, combination treatment further increased the proportion and activation of $CD8^+$ T cells in the 4T1 bone metastasis model (**Figure 6G**), whereas $CD8^+$ T cell activation was enhanced without changes in the proportion in the LLC bone metastasis mice model (**Figure 6J**). NK cell infiltration remained unchanged in both models (**Figure S4D, I**). Furthermore, analysis of the myeloid compartment showed no significant increase in MDSC or DC infiltration (**Figure S4E, F, J, K**). The proportion of $CD101^+$ mature neutrophils was significantly increased following combination treatment (**Figure 6H, K**). Importantly, a more pronounced shift was noted toward M1-like macrophage polarization that was accompanied by a concomitant reduction in M2-like macrophages (**Figures 6I, L and S4G, L**). Together, these findings demonstrated that combining myeloid cell reprogramming with zoledronic acid exerts potent antitumor effects in bone metastasis models by alleviating immune suppression, thereby offering a promising therapeutic strategy for the treatment of bone metastases.

Discussion

In this study myeloid cells within the bone metastasis microenvironment were shown to be crucial for establishing a profoundly immunosuppressive niche. Mechanistically, DKK1-CKAP4 signaling drives neutrophils toward an immature-like functional state, thereby contributing to

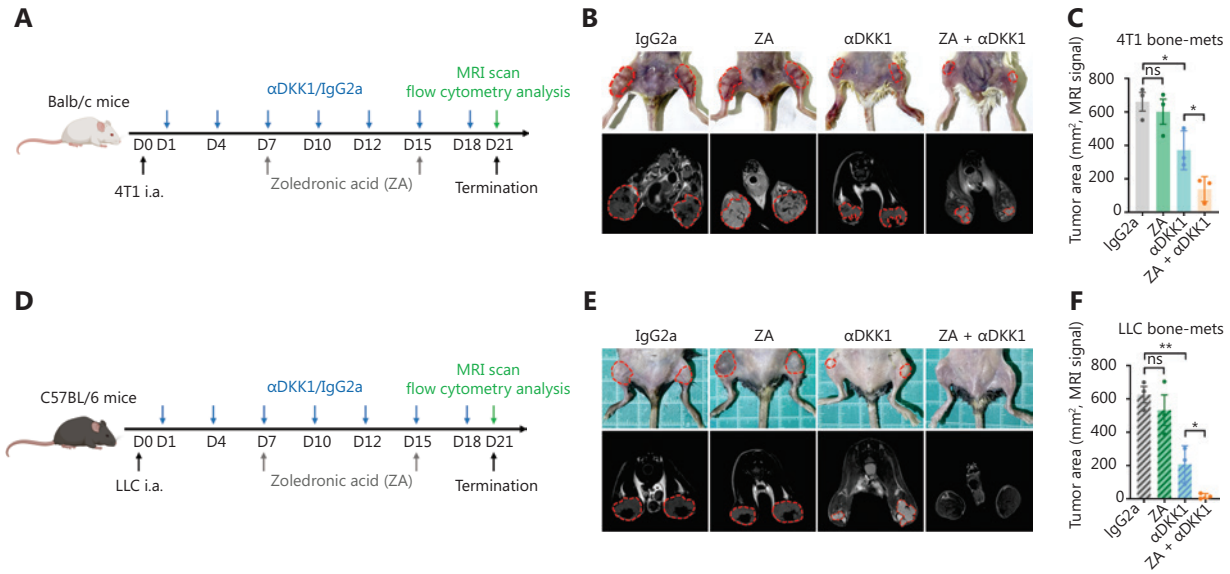


Figure 6 Continued

immunosuppression. DKK1-CKAP4 signaling also promotes osteoclast-like cell differentiation, leading to increased bone destruction. In addition, DKK1-CKAP4 signaling drives polarization of TAMs toward an M2-like state, further reinforcing local immunosuppression. Given previous evidence that DKK1–CKAP4 signaling promotes tumor cell proliferation and survival through activation of the PI3K–AKT pathway, we hypothesize that this pathway may likewise contribute to DKK1–CKAP4-mediated immunosuppressive reprogramming of myeloid cells in the bone TME. Notably, myeloid cell reprogramming combined with zoledronic acid significantly suppressed bone metastasis progression, enhanced $CD8^+$ T cell infiltration and activation, and promoted neutrophil maturation as well as M1 macrophage polarization in the bone TME (**Figure 7**).

Bone metastases exhibit a distinct microenvironment enriched with immunosuppressive myeloid cells, including TANs, osteoclasts and TAMs, which collectively drive tumor progression and therapeutic resistance compared to primary tumor sites[18]. The immune status of neutrophils in bone marrow has a profound impact on tumor growth, metastasis, and response to immunotherapy[19,20]. Extensive studies have focused on the maturation state of TANs, revealing that immature and mature neutrophils may exert heterogeneous functions depending on tumor type and metastasis site. Multi-omics studies and our previous work have shown that the bone metastasis microenvironment is enriched in bone metastasis-bearing mice with $Ly6G^{low}$ $CD101^-$ immature neutrophils, which exhibit strong immunosuppressive activity, whereas $CD101^+$ mature neutrophils in the bone TME do not suppress $CD8^+$ T cell function[21,46-48]. Similar populations of immature neutrophils are also enriched in human cancers both (circulation and tumor sites) and promote immune evasion[48-52]. CXCR2 is a key driver of neutrophil maturation and function in mice. *Cxcr2* deficiency reduces the proportion of mature neutrophils in the spleen and increases the number of $CD62L^{lo}$ $CXCR4^{hi}$ senescent neutrophils[53]. Many solid tumors upregulate CXCL12 and exploit the CXCL12-CXCR4 axis to recruit pathologically activated, immature-like neutrophils, while impairing T cell recruitment, thereby creating an immunosuppressive microenvironment[54]. Consequently, changes in CXCR2 and CXCR4 expression are often used as indicators of neutrophil maturation status. In addition to the immunosuppressive effects mediated by TANs, osteoclasts have a fundamental role in the "vicious cycle," a well-established mechanism underlying bone metastasis[55-57]. A range of osteolysis regulators released by tumor cells, such as RANKL, can activate osteoclasts, which further accelerate bone destruction and release various cytokines, like transforming growth factor-beta (TGF-β), interleukin (IL)-19, and osteopontin (OPN), to promote bone metastases growth[58,59]. Moreover, previous studies have also highlighted the functional heterogeneity of TAMs within the bone metastasis microenvironment. For example, Ma et al. showed that TAMs in breast cancer bone metastases facilitate tumor growth through CCL2-CCR2 and IL4R signaling pathways[25]. Similarly, Li et al. demonstrated that in prostate cancer bone metastases, macrophage-derived activin-A activates the FN1-ITGβ5-SRC axis in tumor cells, contributing to androgen deprivation therapy resistance[26]. Our findings integrate these seemingly distinct observations by identifying DKK1-CKAP4 signaling as a key upstream regulator of this myeloid suppressive network. Rather than acting on a single cell type, DKK1 drives neutrophils toward an immature,

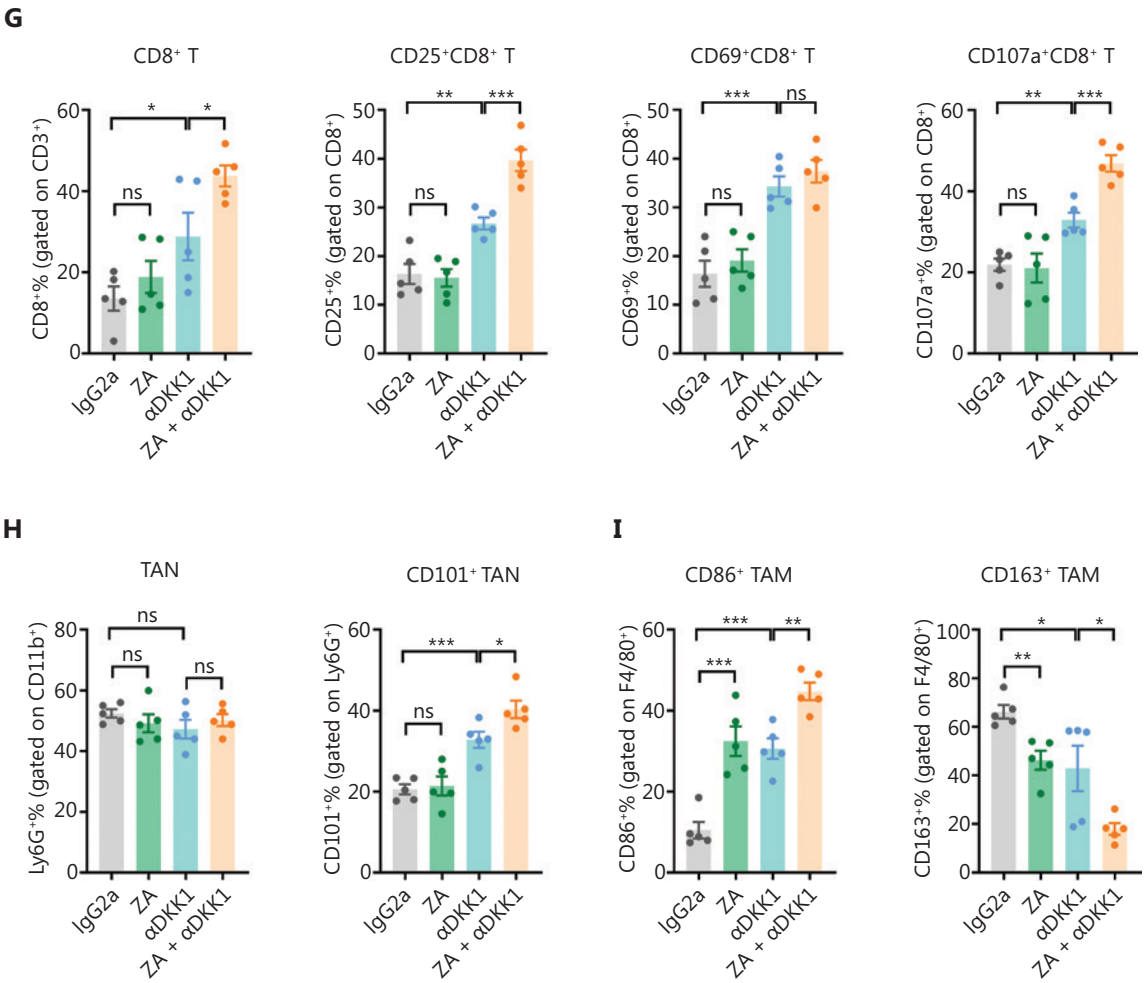


Figure 6 Continued

immunosuppressive phenotype, promotes the differentiation of OCPs toward osteoclast-like cells, and induces macrophage polarization towards an M2-like state. Through these coordinated effects, DKK1 links immune suppression with bone destruction in the bone metastasis microenvironment. This mechanism helps explain how immunosuppression and osteolysis are simultaneously sustained in bone metastases.

As a classic inhibitor of the Wnt signaling pathway, DKK1 competitively binds to the LRP5/6 co-receptors and antagonizes Wnt/β-catenin signaling[60]. By disrupting this pathway, DKK1 contributes to tumor progression, in part by sustaining a poorly differentiated cellular state, which increases malignant behavior[61]. In parallel, DKK1 has also been shown to promote the recruitment and immunosuppressive functions of MDSCs through the same signaling axis, further supporting tumor growth in mouse models[33]. In addition to these canonical effects, recent studies have identified CKAP4 as a non-canonical receptor for DKK1. DKK1-CKAP4 signaling has been implicated in promoting tumor immune evasion at primary tumor sites by directly acting on tumor cells, where DKK1-CKAP4 signaling activates oncogenic pathways, such as PI3K/AKT, and enhances invasive capacity through integrin-mediated adhesion and downstream signaling pathways[27,30,33]. In addition to these tumor-intrinsic effects, accumulating evidence suggests that DKK1 also directly modulates immune cells. Notably, a recent study demonstrated that DKK1 impairs $CD8^+$ T cell-mediated antitumor responses *via* the GSK3β/E2F1/T-bet axis in colorectal cancer models[62], supporting a direct suppressive role of DKK1 on cytotoxic T cells. Our previous findings indicated that the immunosuppressive functions of DKK1 extend beyond direct effects on $CD8^+$ T cells because $CD8^+$ T cell depletion fails to fully abrogate the antitumor efficacy of DKK1 blockade in gastric cancer models[35]. Indeed, DKK1-CKAP4 signaling has been shown to promote M2-like polarization of TAMs in primary tumors, thereby indirectly dampening $CD8^+$ T cell responses[35]. Moreover, our recent study demonstrated that DKK1–CKAP4 signaling activates the PI3K–AKT pathway in neutrophils,

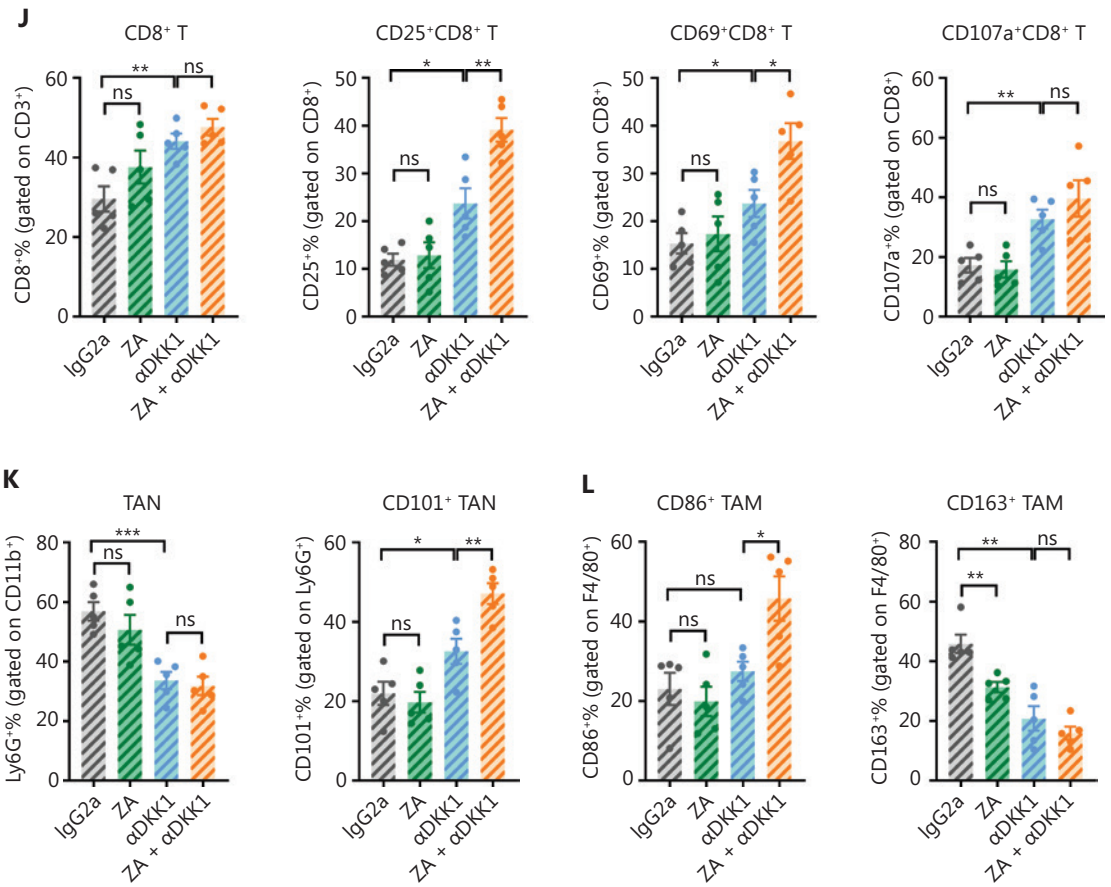


Figure 6 Combining myeloid cell reprogramming with zoledronic acid suppresses tumor progression and remodels the bone metastasis immune microenvironment. (A, D) Schematic of syngeneic breast cancer bone metastasis model (A) or syngeneic lung cancer bone metastasis model (D) and treatment: αDKK1 [10 mg/kg i.p. (7 doses over 3 weeks)] and/or zoledronic acid [100 μg/kg (2 doses)]. (B, E) Representative images and MRI scans of 4T1 (B) or LLC bone metastases (E) at endpoint. (C, F) Quantification of 4T1 (C) or LLC tumor area (F) by MRI. (G-L) Flow cytometry analysis of 4T1 (G–I) and LLC bone metastasis microenvironment (J-L): (G, J) $CD8^+/CD3^+$, $CD25^+/CD8^+$, $CD69^+/CD8^+$, and $CD107a^+/CD8^+$ T cells; (H, K) $Ly6G^+/CD11b^+$ and $CD101^+/Ly6G^+$ neutrophils; (I, L) $CD86^+/F4/80^+$ and $CD163^+/F4/80^+$ macrophages. Bone-mets, bone-metastases; DC, dendritic cell; i.a., intra-arterial; MRI, magnetic resonance imaging; NK, natural kill; TAM, tumor-associated macrophage; TAN, tumor-associated neutrophil; ZA, zoledronic acid; αDKK1, DKK1 antibody. Data are presented as mean ± SEM. ns, not significant, $^*P < 0.05$, $^{**}P < 0.01$, and $^{***}P < 0.001$.

thereby promoting the immunosuppressive functional state[21]. Building on this finding, the present study further reveals that DKK1-CKAP4 signaling broadly reprograms multiple myeloid populations in the bone TME, including TANs, osteoclasts, and TAMs, potentially through activation of the PI3K–AKT pathway, collectively establishing an immunosuppressive microenvironment that constrains $CD8^+$ T cell function. Together, these findings indicate that DKK1 exerts pleiotropic pro-tumor effects by coordinating tumor-intrinsic signaling, directly suppressing cytotoxic T cell activity, and indirectly impairing antitumor immunity through extensive reprogramming of the myeloid compartment, underscoring the potential as a target for combination immunotherapy strategies.

Clinically, accumulating evidence indicates a strong association between DKK1 expression and bone metastasis. A recent study by Zhuang et al. demonstrated that tumor-secreted DKK1 can regulate the organotropism of breast cancer metastasis with high DKK1-expressing tumors preferentially metastasizing to bone, while low DKK1-expressing tumors are more likely to metastasize to the lung[63]. Multiple retrospective studies have further reported that patients with bone metastases from breast, lung, or prostate cancers exhibit significantly elevated DKK1 levels in serum or tumor tissues compared to patients who only have primary tumors[36-38]. Osteoblasts and osteocytes are the most important physiologic source of DKK1, resulting in significantly higher DKK1 concentrations in the bone metastatic microenvironment than in most primary tumor sites[64]. The bone metastatic microenvironment exhibits a distinct cellular composition, characterized by aberrant expansion of myeloid cells, including massive infiltration

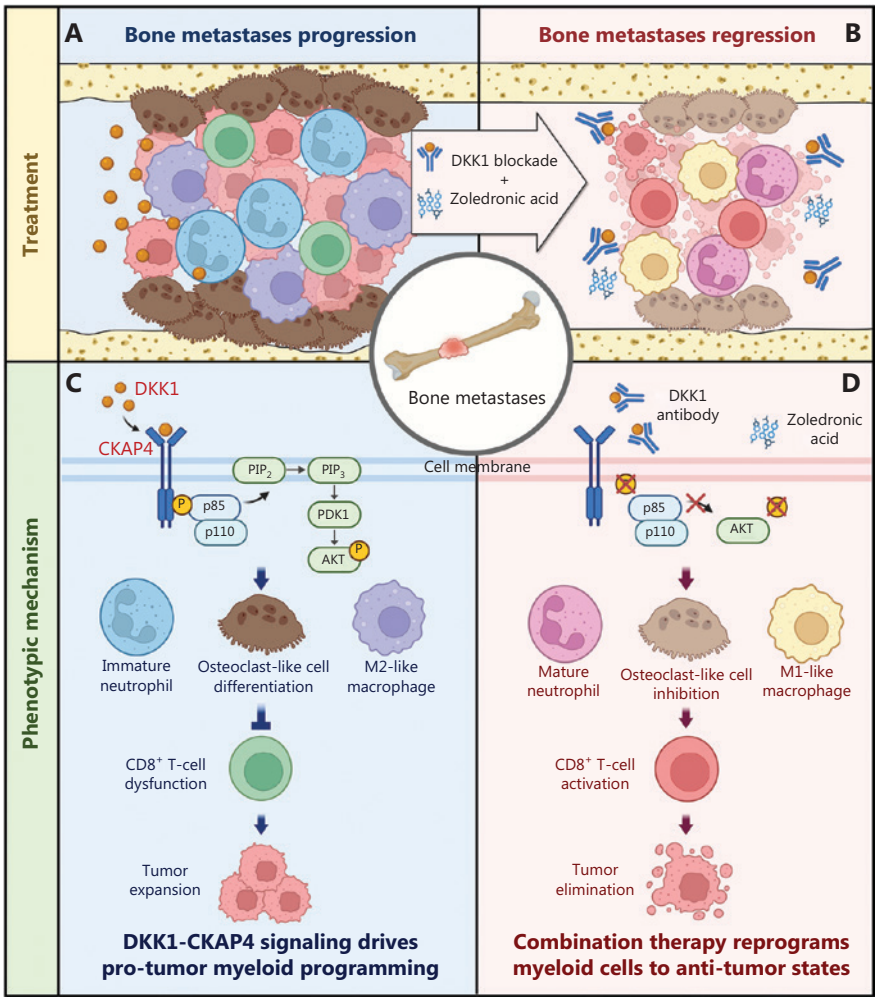


Figure 7 Schematic models illustrating the reprogramming of myeloid cells in the bone metastasis microenvironment combined with zoledronic acid treatment. (A, B) Overall landscape and therapeutic impact. (A) Bone metastases are enriched with immunosuppressive myeloid cell populations, including neutrophils, macrophages, and osteoclasts, which all contribute to the formation of a tumor-promoting microenvironment. **These findings provide a more in-depth understanding of the impact of myeloid cells within the bone metastasis microenvironment.** (B) Therapeutic blockade of DKK1 combined with zoledronic acid reshapes the bone metastasis microenvironment, enhances antitumor immune responses, and suppresses tumor progression. **These findings provide a potential strategy for bone metastasis treatment and broaden the application of zoledronic acid beyond bone protection.** (C, D) Mechanism explanation. (C) Our results derived from neutrophil-specific *Ckap4* knockout mice and *ex vivo* assays demonstrated that the DKK1-CKAP4 signaling axis drives the immunosuppressive and pro-tumorigenic functional states of myeloid cells in the bone metastasis microenvironment, including an immature-like neutrophil state, the differentiation of OCPs toward osteoclast-like cells, and M2-like macrophage polarization. Mechanistically, we hypothesize that DKK1-CKAP4 signaling activates the downstream PI3K–AKT pathway, thereby reinforcing myeloid-mediated immunosuppression, impairing $CD8^+$ T-cell function, and facilitating immune evasion. (D) DKK1 blockade plus zoledronic acid could inhibit the DKK1-CKAP4-PI3K-AKT signaling axis, reprogram myeloid cell function, re-activate $CD8^+$ T cells, and restore antitumor immunity. **These findings uncover the underlying mechanism modulating myeloid cell function within the bone metastasis microenvironment and provide the mechanistic rationale for the combination therapy of DKK1 blockade and zoledronic acid in bone-metastatic patients.** CKAP4, cytoskeleton-associated protein 4; DKK1, dickkopf-1. Figure created with BioRender.com.

of immunosuppressive neutrophils, osteoclasts, and M2-like macrophages. Therefore, the DKK1-CKAP4 signaling axis may have a more critical role in the bone TME compared to primary tumors. The single-cell dataset, GSE143791, was analyzed to further explore the clinical relevance of CKAP4 in the bone metastasis microenvironment. Notably, *CKAP4* expression was markedly elevated in tumor site samples compared to uninvolved or benign bone marrow and this

expression was predominantly restricted to myeloid cell populations. Moreover, *CKAP4*-high myeloid cells exhibited an immunosuppressive signature, which is characterized by high expression of inhibitory molecules (e.g., LGALS9, LILRB3, and S100A8) with low expression of antigen presentation signatures compared to *CKAP4*-low myeloid cells. These human data are consistent with our experimental findings in mouse models. Building on these findings, our data demonstrated that DKK1-CKAP4 signaling is also essential for shaping the bone metastasis microenvironment. Specifically, this axis regulates myeloid cell differentiation and function, thereby promoting a sustained immunosuppressive niche. Together, these results indicated that DKK1-CKAP4 signaling not only drives primary tumor progression but also actively contributes to the establishment of the bone metastasis environment.

Despite the availability of multiple therapeutic strategies for primary tumors[65,66], effective treatments for bone metastases are limited. Chemotherapy, radiotherapy, and immunotherapies generally elicit unsatisfactory responses in this setting[13,15,17]. Given the profoundly immunosuppressive microenvironment of bone metastases, monotherapy is often insufficient, making combination therapy particularly important. Recent studies have demonstrated progress in the treatment of bone metastases using conventional bone-protective agents and myeloid reprogramming therapies. For example, osteoclast-derived OPN mediates systemic resistance to ICB and combining ICB with an anti-RANKL antibody effectively blocks osteoclastogenesis and restores ICB efficacy[24]. Strategies co-targeting T cells and myeloid cells have also made important progress. For example, concurrent blockade of TIGIT on T cells and IL-1β produced by myeloid cells in a breast cancer bone metastasis model effectively activated antitumor immunity, suppressed bone metastases, and improved survival[67]. These studies indicated that conventional bone-protective agents possess therapeutic potential and targeting myeloid cells represents a critical component of immunotherapy within the bone metastatic microenvironment. Zoledronic acid, as another commonly used bone-protective agent, is a standard treatment for patients with bone metastases and is widely used in clinical practice to prevent SREs[12]. However, the impact on overall survival remains limited, highlighting the need for more effective combination therapies[7,9,68-70]. In addition to bone-protective effects, zoledronic acid has been reported to exert modest immunomodulatory activity. Preclinical studies have shown that zoledronic acid partially induces M1-like polarization of macrophages and suppresses M2-associated markers, suggesting a potential role in modulating the TME[71]. Nevertheless, these effects appear insufficient to reverse the profound immunosuppression observed in bone metastases, suggesting that combining zoledronic acid with myeloid reprogramming may hold therapeutic promise. In this study we found that combining myeloid reprogramming with zoledronic acid markedly enhanced the recruitment and activation of $CD8^+$ T cells, drove neutrophil maturation, and promoted macrophage polarization toward the M1 phenotype within the TME, thereby exerting potent antitumor effects. Notably, the DKK1-neutralizing antibody, DKN-01, has already shown encouraging clinical activity in primary tumor sites[72,73], supporting the translational potential of this combination strategy for patients with bone metastases. Taken together, our findings demonstrated that zoledronic acid, when combined with myeloid reprogramming, functions not only as a bone-protective agent but also an effective drug for tumor control. This combination markedly improves the antitumor activity of a widely used clinical drug and extends the role from preventing skeletal-related events to actively suppressing tumor progression in bone metastases.

Our study had several limitations. First, we only used two syngeneic murine bone metastases models (4T1 and LLC), which may not fully reflect the heterogeneity of metastatic disease across diverse tumor types. Second, our findings have not been validated in clinical samples, so corollary studies should include analyses of bone metastasis from patients to confirm the translational relevance of these findings. In addition, although we investigated the effects of DKK1 on neutrophils, osteoclast-like cells, and macrophages in bone TME, the precise downstream signaling pathways involved in DKK1–CKAP4-mediated immune modulation remain to be explored. Finally, the potential contribution of canonical DKK1 receptors (LRP5/6) to immune regulation within the bone TME was not addressed in this study and whether these classical pathways cooperate with or compensate for CKAP4-dependent signaling warrants further investigation.

Conclusions

In summary, this study highlights the critical impact of myeloid cells in the bone TME and identifies a potential regulatory mechanism underlying immunosuppressive functions. Furthermore, we proposed a novel combination strategy with promising translational potential for bone metastases.

Grant support

This work was funded by grants from the National Major Projects for 'Major New Drugs Innovation and Development' (2025ZD1800302), the Fundamental and Interdisciplinary Disciplines Breakthrough Plan of the Ministry of Education of China (JYB2025XDXM501), the National Natural Science Foundation of China (82373263 and 82403835), the China Postdoctoral Science Foundation (2024M751405), the Jiangsu Provincial Natural Science Foundation Youth Project (BK20240247), and the Fundamental Research Funds for the Central Universities (2026300385). The funding sources had

no role in the study design, data collection, data analysis, data interpretation, or writing of the manuscript.

Conflict of interest statement

No potential conflicts of interest are disclosed.

Author contributions

Conceived and designed the analysis: Jia Wei, Tao Shi.
Collected the data: Yiran Cai, Zizheng Jiang, Ke Zheng.
Contributed data or analysis tools: Jia Wei, Lixia Yu, Baorui Liu.
Performed the analysis: Yuting Luo, Shiji Ren.
Wrote the paper: Yuting Luo, Tao Shi.

Data availability statement

The data generated in this study are available upon request from the corresponding author.

References

1. Coleman RE, Croucher PI, Padhani AR, Clézardin P, Chow E, Fallon M, et al. Bone metastases. Nat Rev Dis Primers 2020; 6: 83.
2. Siegel RL, Kratzer TB, Giaquinto AN, Sung H, Jemal A. Cancer statistics, 2025. CA Cancer J Clin. 2025; 75: 10-45.
3. Coleman RE. Clinical features of metastatic bone disease and risk of skeletal morbidity. Clin Cancer Res. 2006; 12: 6243s-49s.
4. D'Oronzo S, Coleman R, Brown J, Silvestris F. Metastatic bone disease: pathogenesis and therapeutic options. J Bone Oncol. 2019; 15: 100205.
5. Clézardin P, Coleman R, Puppo M, Ottewell P, Bonnelye E, Paycha F, et al. Bone metastasis: mechanisms, therapies, and biomarkers. Physiol Rev. 2021; 101: 797-855.
6. Mollica V, Rizzo A, Rosellini M, Marchetti A, Ricci AD, Cimadamore A, et al. Bone targeting agents in patients with metastatic prostate cancer: state of the art. Cancers (Basel). 2021; 13: 546.
7. Early Breast Cancer Trialists' Collaborative Group (EBCTCG). Adjuvant bisphosphonate treatment in early breast cancer: meta-analyses of individual patient data from randomised trials. Lancet. 2015; 386: 1353-61.
8. Fizazi K, Foulon S, Carles J, Roubaud G, McDermott R, Fléchon A, et al. Abiraterone plus prednisone added to androgen deprivation therapy and docetaxel in de novo metastatic castration-sensitive prostate cancer (PEACE-1): a multicentre, open-label, randomised, phase 3 study with a 2 × 2 factorial design. Lancet. 2022; 399: 1695-707.
9. Fizazi K, Carducci M, Smith M, Damião R, Brown J, Karsh L, et al. Denosumab versus zoledronic acid for treatment of bone metastases in men with castration-resistant prostate cancer: a randomised, double-blind study. Lancet. 2011; 377: 813-22.
10. Gnant M, Pfeiler G, Steger GG, Egle D, Greil R, Fitzal F, et al. Adjuvant denosumab in postmenopausal patients with hormone receptor-positive breast cancer (ABCSG-18): disease-free survival results from a randomised, double-blind, placebo-controlled, phase 3 trial. Lancet Oncol. 2019; 20: 339-51.
11. Peters S, Danson S, Hasan B, Dafni U, Reinmuth N, Majem M, et al. A randomized open-label phase III trial evaluating the addition of denosumab to standard first-line treatment in advanced NSCLC: the European Thoracic Oncology Platform (ETOP) and European Organisation for Research and Treatment of Cancer (EORTC) SPLENDOUR trial. J Thorac Oncol. 2020; 15: 1647-56.
12. von Moos R, Costa L, Gonzalez-Suarez E, Terpos E, Niepel D, Body JJ. Management of bone health in solid tumours: from bisphosphonates to a monoclonal antibody. Cancer Treat Rev. 2019; 76: 57-67.
13. Reinstein ZZ, Pamarthy S, Sagar V, Costa R, Abdulkadir SA, Giles FJ, et al. Overcoming immunosuppression in bone metastases. Crit Rev Oncol Hematol. 2017; 117: 114-27.
14. Beer TM, Kwon ED, Drake CG, Fizazi K, Logothetis C, Gravis G, et al. Randomized, double-blind, phase III trial of ipilimumab versus placebo in asymptomatic or minimally symptomatic patients with metastatic chemotherapy-naive castration-resistant prostate cancer. J Clin Oncol. 2017; 35: 40-7.
15. Sharma P, Pachynski RK, Narayan V, Fléchon A, Gravis G, Galsky MD, et al. Nivolumab plus ipilimumab for metastatic castration-resistant prostate cancer: preliminary analysis of patients in the CheckMate 650 trial. Cancer Cell. 2020; 38: 489-99.e3.
16. Jiao S, Subudhi SK, Aparicio A, Ge Z, Guan B, Miura Y, et al. Differences in tumor microenvironment dictate T helper lineage polarization and response to immune checkpoint therapy. Cell. 2019; 179: 1177-90.e13.
17. Wang K, Gu Y, Liao Y, Bang S, Donnelly CR, Chen O, et al. PD-1 blockade inhibits osteoclast formation and murine bone cancer pain. J Clin Invest. 2020; 130: 3603-20.
18. Jackett KN, Browne AT, Aber ER, Clements M, Kaplan RN. How the bone microenvironment shapes the pre-metastatic niche and metastasis. Nat Cancer. 2024; 5: 1800-14.
19. Gungabeesoon J, Gort-Freitas NA, Kiss M, Bolli E, Messemaker M, Siwicki M, et al. A neutrophil response linked to tumor control in immunotherapy. Cell. 2023; 186: 1448-64.e20.
20. Hirschhorn D, Budhu S, Kraehenbuehl L, Gigoux M, Schröder D, Chow A, et al. T cell immunotherapies engage neutrophils to eliminate tumor antigen escape variants. Cell. 2023; 186: 1432-47.e17.
21. Shi T, Liu W, Luo Y, Liang K, Ren S, Song X, et al. CHI3L3^{+} immature neutrophils inhibit anti-tumor immunity and impede immune checkpoint blockade therapy in bone metastases. Cancer Cell. 2025; 43: 1937-57.e11.
22. He Y, Luo W, Liu Y, Wang Y, Ma C, Wu Q, et al. IL-20RB mediates tumoral response to osteoclastic niches and promotes bone metastasis of lung cancer. J Clin Invest. 2022; 132: e157917.

23. Yue Z, Niu X, Yuan Z, Qin Q, Jiang W, He L, et al. RSPO2 and RANKL signal through LGR4 to regulate osteoclastic premetastatic niche formation and bone metastasis. J Clin Invest. 2022; 132: e144579.
24. Cheng JN, Jin Z, Su C, Jiang T, Zheng X, Guo J, et al. Bone metastases diminish extraosseous response to checkpoint blockade immunotherapy through osteopontin-producing osteoclasts. Cancer Cell. 2025; 43: 1093-107.e9.
25. Ma RY, Zhang H, Li XF, Zhang CB, Selli C, Tagliavini G, et al. Monocyte-derived macrophages promote breast cancer bone metastasis outgrowth. J Exp Med. 2020; 217: e20191820.
26. Li XF, Selli C, Zhou HL, Cao J, Wu S, Ma RY, et al. Macrophages promote anti-androgen resistance in prostate cancer bone disease. J Exp Med. 2023; 220: e20221007.
27. Kimura H, Fumoto K, Shojima K, Nojima S, Osugi Y, Tomihara H, et al. CKAP4 is a Dickkopf1 receptor and is involved in tumor progression. J Clin Invest. 2016; 126: 2689-705.
28. Li MH, Dong LW, Li SX, Tang GS, Pan YF, Zhang J, et al. Expression of cytoskeleton-associated protein 4 is related to lymphatic metastasis and indicates prognosis of intrahepatic cholangiocarcinoma patients after surgery resection. Cancer Lett. 2013; 337: 248-53.
29. Nagoya A, Sada R, Kimura H, Yamamoto H, Morishita K, Miyoshi E, et al. CKAP4 is a potential exosomal biomarker and therapeutic target for lung cancer. Transl Lung Cancer Res. 2023; 12: 408-26.
30. Liu Z, Chen M, Xie LK, Liu T, Zou ZW, Li Y, et al. CLCA4 inhibits cell proliferation and invasion of hepatocellular carcinoma by suppressing epithelial-mesenchymal transition via PI3K/AKT signaling. Aging (Albany NY). 2018; 10: 2570-84.
31. Osugi Y, Fumoto K, Kikuchi A. CKAP4 regulates cell migration via the interaction with and recycling of integrin. Mol Cell Biol. 2019; 39: e00073-19.
32. Li SX, Tang GS, Zhou DX, Pan YF, Tan YX, Zhang J, et al. Prognostic significance of cytoskeleton-associated membrane protein 4 and its palmitoyl acyltransferase DHHC2 in hepatocellular carcinoma. Cancer. 2014; 120: 1520-31.
33. D'Amico L, Mahajan S, Capietto AH, Yang Z, Zamani A, Ricci B, et al. Dickkopf-related protein 1 (Dkk1) regulates the accumulation and function of myeloid derived suppressor cells in cancer. J Exp Med. 2016; 213: 827-40.
34. Haas MS, Kagey MH, Heath H, Schuerpf F, Rottman JB, Newman W. mDKN-01, a novel anti-DKK1 mAb, enhances innate immune responses in the tumor microenvironment. Mol Cancer Res. 2021; 19: 717-25.
35. Shi T, Zhang Y, Wang Y, Song X, Wang H, Zhou X, et al. DKK1 promotes tumor immune evasion and impedes anti–PD-1 treatment by inducing immunosuppressive macrophages in gastric cancer. Cancer Immunol Res. 2022; 10: 1506-24.
36. Chu T, Teng J, Jiang L, Zhong H, Han B. Lung cancer-derived Dickkopf1 is associated with bone metastasis and the mechanism involves the inhibition of osteoblast differentiation. Biochem Biophys Res Commun. 2014; 443: 962-8.
37. Kasoha M, Bohle RM, Seibold A, Gerlinger C, Juhasz-Böss I, Solomayer EF. Dickkopf-1 (Dkk1) protein expression in breast cancer with special reference to bone metastases. Clin Exp Metastasis. 2018; 35: 763-75.
38. Yuan S, Hoggard NK, Kantake N, Hildreth BE 3rd, Rosol TJ. Effects of Dickkopf-1 (DKK-1) on prostate cancer growth and bone metastasis. Cells. 2023; 12: 2695.
39. Cossarizza A, Chang HD, Radbruch A, Abrignani S, Addo R, Akdis M, et al. Guidelines for the use of flow cytometry and cell sorting in immunological studies (third edition). Eur J Immunol. 2021; 51: 2708-3145.
40. He LH, Liu M, He Y, Xiao E, Zhao L, Zhang T, et al. TRPV1 deletion impaired fracture healing and inhibited osteoclast and osteoblast differentiation. Sci Rep. 2017; 7: 42385.
41. Kuchimaru T, Kataoka N, Nakagawa K, Isozaki T, Miyabara H, Minegishi M, et al. A reliable murine model of bone metastasis by injecting cancer cells through caudal arteries. Nat Commun. 2018; 9: 2981.
42. Sun X, Park MD, Merad M, Brown BD. Macrophages: targets for next-generation cancer immunotherapy. Cancer Cell. 2026; 44: 498-518.
43. Baş Y. Is the "PD-L1 macrophage score" possible as an immunotherapy target in colon adenocarcinoma? Gastrointest Tumors. 2024; 11: e003.
44. Zhu C, Kong Z, Wang B, Cheng W, Wu A, Meng X. ITGB3/CD61: a hub modulator and target in the tumor microenvironment. Am J Transl Res. 2019; 11: 7195-208.
45. Husheem M, Nyman JK, Vaaraniemi J, Vaananen HK, Hentunen TA. Characterization of circulating human osteoclast progenitors: development of in vitro resorption assay. Calcif Tissue Int. 2005; 76: 222-30.
46. Dinh HQ, Eggert T, Meyer MA, Zhu YP, Olingy CE, Llewellyn R, et al. Coexpression of CD71 and CD117 identifies an early unipotent neutrophil progenitor population in human bone marrow. Immunity. 2020; 53: 319-34.e6.
47. Xie X, Shi Q, Wu P, Zhang X, Kambara H, Su J, et al. Single-cell transcriptome profiling reveals neutrophil heterogeneity in homeostasis and infection. Nat Immunol. 2020; 21: 1119-33.
48. Liu W, Shi T, Lu C, Che K, Zhang Z, Luo Y, et al. Human myelocyte and metamyelocyte-stage neutrophils suppress tumor immunity and promote cancer progression. Cell Res. 2025; 35: 588-606.
49. Gong Z, Li Q, Shi J, Li P, Hua L, Shultz LD, et al. Immunosuppressive reprogramming of neutrophils by lung mesenchymal cells promotes breast cancer metastasis. Sci Immunol. 2023; 8: eadd5204.
50. Evrard M, Kwok IWH, Chong SZ, Teng KWW, Becht E, Chen J, et al. Developmental analysis of bone marrow neutrophils reveals populations specialized in expansion, trafficking, and effector functions. Immunity. 2018; 48: 364-79.e8.
51. Sagiv JY, Michaeli J, Assi S, Mishalian I, Kisos H, Levy L, et al. Phenotypic diversity and plasticity in circulating neutrophil subpopulations in cancer. Cell Rep. 2015; 10: 562-73.
52. Rice CM, Davies LC, Subleski JJ, Maio N, Gonzalez-Cotto M, Andrews C, et al. Tumour-elicited neutrophils engage mitochondrial metabolism to circumvent nutrient limitations and maintain immune suppression. Nat Commun. 2018; 9: 5099.

53. Delobel P, Ginter B, Rubio E, Balabanian K, Lazennec G. CXCR2 intrinsically drives the maturation and function of neutrophils in mice. Front Immunol. 2022; 13: 1005551.
54. Qian J, Ma C, Waterbury QT, Zhi X, Moon CS, Tu R, et al. A CXCR4 partial agonist improves immunotherapy by targeting immunosuppressive neutrophils and cancer-driven granulopoiesis. Cancer Cell. 2025; 43: 1512-29.e11.
55. Mundy GR. Mechanisms of bone metastasis. Cancer. 1997; 80: 1546-56.
56. Guise TA, Kozlow WM, Heras-Herzig A, Padalecki SS, Yin JJ, Chirgwin JM. Molecular mechanisms of breast cancer metastases to bone. Clin Breast Cancer. 2005; 5: S46-53.
57. Fornetti J, Welm AL, Stewart SA. Understanding the bone in cancer metastasis. J Bone Miner Res. 2018; 33: 2099-113.
58. Nakashima T, Hayashi M, Fukunaga T, Kurata K, Oh-Hora M, Feng JQ, et al. Evidence for osteocyte regulation of bone homeostasis through RANKL expression. Nat Med. 2011; 17: 1231-34.
59. Waning DL, Mohammad KS, Reiken S, Xie W, Andersson DC, John S, et al. Excess TGF-β mediates muscle weakness associated with bone metastases in mice. Nat Med. 2015; 21: 1262-71.
60. Kagey MH, He X. Rationale for targeting the Wnt signalling modulator Dickkopf-1 for oncology. Br J Pharmacol. 2017; 174: 4637-50.
61. Goldstein SD, Trucco M, Bautista Guzman W, Hayashi M, Loeb DM. A monoclonal antibody against the Wnt signaling inhibitor dickkopf-1 inhibits osteosarcoma metastasis in a preclinical model. Oncotarget. 2016; 7: 21114-23.
62. Sui Q, Liu D, Jiang W, Tang J, Kong L, Han K, et al. Dickkopf 1 impairs the tumor response to PD-1 blockade by inactivating CD8+ T cells in deficient mismatch repair colorectal cancer. J Immunother Cancer. 2021; 9: e001498.
63. Zhuang X, Zhang H, Li X, Li X, Cong M, Peng F, et al. Differential effects on lung and bone metastasis of breast cancer by Wnt signalling inhibitor DKK1. Nat Cell Biol. 2017; 19: 1274-85.
64. Ke HZ, Richards WG, Li X, Ominsky MS. Sclerostin and Dickkopf-1 as therapeutic targets in bone diseases. Endocr Rev. 2012; 33: 747-83.
65. Takahashi N, Umezawa R, Yamamoto T, Takeda K, Suzuki Y, Kishida K, et al. A retrospective study of clinical outcomes for patients with esophageal cancer who were treated with radiotherapy alone. Gastrointest Tumors. 2024; 10: 57-66.
66. Xu J, Yan D, Hu R, Zhang S, Jiang X. Surgical decisions and quality of life after gastrectomy for gastric cancer: update from Asian studies. Gastrointest Tumors. 2024; 11: e002.
67. Monteran L, Ershaid N, Scharff Y, Zoabi Y, Sanalla T, Ding Y, et al. Combining TIGIT blockade with MDSC inhibition hinders breast cancer bone metastasis by activating antitumor immunity. Cancer Discov. 2024; 14: 1252-75.
68. Barrett-Lee P, Casbard A, Abraham J, Hood K, Coleman R, Simmonds P, et al. Oral ibandronic acid versus intravenous zoledronic acid in treatment of bone metastases from breast cancer: a randomised, open label, non-inferiority phase 3 trial. Lancet Oncol. 2014; 15: 114-22.
69. Smith MR, Halabi S, Ryan CJ, Hussain A, Vogelzang N, Stadler W, et al. Randomized controlled trial of early zoledronic acid in men with castration-sensitive prostate cancer and bone metastases: results of CALGB 90202 (alliance). J Clin Oncol. 2014; 32: 1143-50.
70. Henry DH, Costa L, Goldwasser F, Hirsh V, Hungria V, Prausova J, et al. Randomized, double-blind study of denosumab versus zoledronic acid in the treatment of bone metastases in patients with advanced cancer (excluding breast and prostate cancer) or multiple myeloma. J Clin Oncol. 2011; 29: 1125-32.
71. Weber M, Homm A, Muller S, Frey S, Amann K, Ries J, et al. Zoledronate causes a systemic shift of macrophage polarization towards M1 in vivo. Int J Mol Sci. 2021; 22: 1323.
72. Klempner SJ, Sonbol MB, Wainberg ZA, Uronis HE, Chiu VK, Scott AJ, et al. DKN-01 in combination with tislelizumab and chemotherapy as first-line therapy in advanced gastric or gastroesophageal junction adenocarcinoma: DisTinGuish. J Clin Oncol. 2025; 43: 339-49.
73. Shi T, Wei J. Targeting DKK1 to remodel the tumor microenvironment and enhance immune checkpoint blockade therapy. J Clin Oncol. 2025; 43: 350-3.

Cite this article as: Luo Y, Cai Y, Jiang Z, Zheng K, Ren S, Yu L, et al. Myeloid cell reprogramming combined with zoledronic acid effectively suppresses bone metastasis. Cancer Biol Med. 2026; 23: 1167-1192. doi: 10.20892/j.issn.2095-3941.2026.0168